The Effect of Aging on the Fatigue Strength of Alloy 800HT

by

Fathi Hussain Al-Habib

A Thesis Presented to the

FACULTY OF THE COLLEGE OF GRADUATE STUDIES

KING FAHD UNIVERSITY OF PETROLEUM & MINERALS

DHAHRAN, SAUDI ARABIA

In Partial Fulfillment of the
Requirements for the Degree of

MASTER OF SCIENCE

In

MECHANICAL ENGINEERING

September, 1999

INFORMATION TO USERS

This manuscript has been reproduced from the microfilm master. UMI films the text directly from the original or copy submitted. Thus, some thesis and dissertation copies are in typewriter face, while others may be from any type of computer printer.

The quality of this reproduction is dependent upon the quality of the copy submitted. Broken or indistinct print, colored or poor quality illustrations and photographs, print bleedthrough, substandard margins, and improper alignment can adversely affect reproduction.

In the unlikely event that the author did not send UMI a complete manuscript and there are missing pages, these will be noted. Also, if unauthorized copyright material had to be removed, a note will indicate the deletion.

Oversize materials (e.g., maps, drawings, charts) are reproduced by sectioning the original, beginning at the upper left-hand corner and continuing from left to right in equal sections with small overlaps.

Photographs included in the original manuscript have been reproduced xerographically in this copy. Higher quality 6" x 9" black and white photographic prints are available for any photographs or illustrations appearing in this copy for an additional charge. Contact UMI directly to order.

Bell & Howell Information and Learning
300 North Zeeb Road, Ann Arbor, MI 48106-1346 USA

UMI®
800-521-0600

THE EFFECT OF AGING ON THE FATIGUE STRENGTH OF ALLOY 800HT

BY

FATHI HUSSAIN ALHABIB

A Thesis Presented to the

DEANSHIP OF GRADUATE STUDIES

KING FAHD UNIVERSITY OF PETROLEUM & MINERALS

DHAHRAN, SAUDI ARABIA

In Partial Fulfillment of the
Requirements for the Degree of

MASTER OF SCIENCE

In

MECHANICAL ENGINEERING

September, 1999

UMI Number: 1397407

UMI Microform 1397407

Bell & Howell Information and Learning Company
300 North Zeeb Road
P.O. Box 1346
Ann Arbor, MI 48106-1346

KING FAHD UNIVERSITY OF PETROLEUM AND MINERALS
DHAHRAN 31261, SAUDI ARABIA

DEANSHIP OF GRADUATE STUDIES

This thesis, written by

Fathi Hussain Al-Habib

under the direction of his Thesis Advisor and approved by his Thesis Committee, has been presented to and approved by the Dean of Graduate Studies, in partial fulfillment of the requirement for the degree of

MASTER OF SCIENCE IN MECHANICAL ENGINEERING

Thesis Committee

Dr. Zafarullah Khan (Chairman)

Dr. Ibrahim Allam (member)

Dr. Necar Merah (Member)

Dr. John Shirokoff (Member)

25/9/1999

Department Chairman (Mechanical Engineering)

Dean of Graduate Studies

25/9/99

Date

This thesis is dedicated to

my wife Zahra

who always stood beside me and, after the wish of ALLAH, made this effort possible.

ACKNOWLEDGMENT

Acknowledgment is due to King Fahd University of Petroleum and Minerals for support of this research. My thanks are due to the Mechanical Engineering Department for the use of the experimental facilities of the Department.

I wish to express my appreciation to Dr. Zafarlullah Khan who served as my thesis advisor for his support, patience and guidance. I also wish to thank the other members of my thesis committee, Dr. Necar Merah, Dr. Ibrahin Allam, and Dr. John Shirokoff for their contribution.

My appreciation is also due to Mr. Zainulaudin, of the Advanced Material Laboratory, who was very helpful in assisting in the experimental work.

TABLE OF CONTENT

LIST OF TABLES

LIST OF FIGURES

ABSTRACT

NAME: FATHI HUSSAIN AL-HABIB.

TITLE: THE EFFECT OF AGING ON THE FATIGUE STRENGTH OF ALLOY 800HT

MAJOR FIELD: MECHANICAL ENGINEERING

DATE OF DEGREE: September, 1999

Alloy 800HT is a heat resistance material that is used in high temperature industrial applications such as steam/hydrocarbon reforming and ethylene plant tubes. Long time exposure under these service conditions cause the alloy to undergo microstructural changes. The alloy, in fact, is subjected to an in-service aging process. These in-service microstructural changes, thus, among other effects, are expected to have a pronounced effect on the fatigue strength of this alloy. This study explores the effect of the aging treatment on the fatigue strength of alloy 800 HT. In-service aging-induced microstructural changes are simulated by pre-aging the alloy specimens prior to fatigue testing. This study has revealed that the inter-granular and intra-granular precipitates, formed during the aging treatment, have a significant effect on the fatigue resistance of the alloy.

High temperature aging is observed to promote the formation of coarse grain boundary, twin boundary as well as intra-granular $M_{23}C_6$ type precipitates. These precipitate particles were also observed to reduce the alloy fatigue strength by promoting the fatigue crack initiation and propagation. Compared to the temperature effect, the aging time is observed to be not as effective in influencing the material fatigue strength. Microstructural examinations have also revealed that fatigue cracks were predominantly trans-granular in the crack initiation and propagation regions, and with rough surfaces for the high temperature aged specimens.

Master Of Science Degree
Department of Mechanical Engineering
KING FAHD UNIVERSITY OF PETROLEUM AND MINERALS
Dhahran, Saudi Arabia
September, 1999

خلاصة الرسالة

الاسم	:	فتحي حسين محمد الحبيب
عنوان الدراسة	:	تأثير المعالجة الحرارية على مقاومة الإجهاد للمادة Alloy 800HT
التخصص	:	الهندسة الميكانيكية
تاريخ الشهادة	:	سبتمبر – ١٩٩٩م

تستخدم السبيكة المعدنية من نوع Alloy 800HT في تطبيقات صناعية مختلفة في المفاعل النووي وكيماوية المعاصرة و تعتبر من المواد المقاومة لدرجات الحرارة العالية. إن تعريض هذه المادة لمستويات عالية من الحرارة و لفترات متطاولة يؤدي لحدوث تغيرات في البنية المجهرية (Microstructure) لهذه المادة مما قد يؤثر على قوة المقاومة لهذه المادة لحالة الإجهاد (Fatigue). تقوم هذه الدراسة على استكشاف تأثير مقاومة الإجهاد في المادة Alloy 800HT بالتعريض لدرجات الحرارة العالية و ذلك عن طريق إجراء اختبار تحديد قوة مقاومة الإجهاد (Fatigue Strength) بعد تسخين هذه المادة إلى مستويات محددة من درجات الحرارة تؤدي إلى حدوث تغيرات في البنية المجهرية (Microstructure). لقد تبين من خلال هذه الدراسة أن الترسبات الحاصلة في البنية المجهرية و الناتجة عن التعرض للحرارة لها تأثير واضح في قوة المعدن لمقاومة الإجهاد . ان حالة التعمير الحاصل لهذه المادة و الناتج عن تعريضها لدرجات حرارة عالية يساعد على تسريع تكوين ترسبات من نوع $M_{23}C_6$ في البنية المجهرية و إن ذلك الترسب يخفض من مستوى مقاومة المادة للإجهاد من خلال المساعدة على تكوين و نمو الشروخ الإجهادية.

درجة الماجستير في العلوم

قسم الهندسة الميكانيكية

جامعة الملك فهد للبترول و المعادن

الظهران – المملكة العربية السعودية

سبتمبر – ١٩٩٩م

CHAPTER 1

INTRODUCTION

1.1 GENERAL:

INCOLOY 800HT is an exceptionally useful material in elevated temperature applications and curburizing/oxidizing corrosive environments. This wrought alloy is widely used as a construction material in chemical, petrochemical, nuclear power plants, and a number of other industrial applications. It has an extensive use in the petrochemical and chemical process industries where high temperature corrosion resistance is essential and has shown excellent resistance to such environments [1]. In these industries alloy 800HT has been extensively used in a wide range of applications such as steam/hydrocarbon reforming as catalyst tubing, convection section tubing, pigtails, outlet headers, and transfer line mains. In ethylene plants, the alloy is being used in both convection and cracking tubes, while in hydrodealkylation units in oxo-alcohol production plants the alloy is used as heater tubes[2]. Radiant tubes, muffles, retorts, and assorted furnace fixture are some more applications found in industrial heating equipment. The alloy is also used as a material for heat-exchanging components in various energy conversion systems.

In such applications, the components are normally subjected to high cycle fatigue caused by vibration or oscillation, which could occur due to mechanical or fluid flow excitations. The alloy is also subjected to low cycle fatigue caused by thermal cycling coupled with long exposure to high temperature creep conditions. Fatigue condition could also occur due to the relative expansion movement of the catalyst tubes away and towards the outlet sub-header during plant start-up and shutdown conditions. This would induce low cycle fatigue conditions. The material, under these environments goes through many microstructural changes that could directly influence the fatigue as well as other mechanical properties. During service the alloy microstructure is believed to experience an aging process where various types of precipitates are formed at the grain/twin boundaries and inside the grain structure depending on the temperature level and exposure time. A proper understanding and characterization of alloy 800HT fatigue behavior as affected by these environment-induced microstructural changes becomes essential for proper component design and reliable functioning and operation of the plant equipment made of alloy 800HT.

Alloy 800HT is an iron based austenitic Nickel super-alloy containing large amounts of Cr and Ni. The alloy is a well-recognized material for having a high strength and its ability to resist corrosion, oxidation, carburization and its excellent fabricability [2]. It was developed as an improved version of Alloy 800, and has an upper carbon content restriction with aluminum plus titanium content of 0.85% minimum. Alloy 800HT

receives an annealing treatment at 1200° C for 10 minutes which produces an average grain size of ASTM number 3.0.

This is designed to give the alloy a better creep and rupture strength that adds to its ability to resist high temperature corrosion, and makes it exceptionally useful in elevated temperature and corrosive environment applications[3]. In fact, this and similar super-alloys have been developed to handle sever work environments where the 300 series stainless steel alloys have shown failure. This alloy also replaces the more expensive nickel based super-alloys.

Alloy 800HT, in the as-received condition, contains austenitic titanium carbo-nitrides[2] randomly distributed inside the grain matrix, but not at the grain or twin boundaries. The microstructure is found to have a certain degree of sensitivity to temperature exposure with regard to the precipitate formation. Carbides start to form at the grain boundaries after exposure to high temperature, and were found to stabilize after 1000 hours of exposure at 650° C or higher temperatures[9]. The carbide network at the grain boundaries was also found to coarsen with long time exposure of high temperatures. The effect of such precipitates on the fatigue strength of alloy 800HT has been studied by a number of researchers during the last decade or two, and is the subject of this study.

In general we can have various types of microstrucural changes in the austenite matrix which will have an influence on the mechanical properties of the alloy. The first being

solid solution hardening which occurs when atoms of alloying elements such as molybdenum and tungsten diffuse and scatter evenly into the nickel base metal. Such a phenomenon is a slow process and occurs at high temperature reaching 60% of the metal melting temperature and leads to an increase in the alloy tensile strength[4].

Although nickel is generally considered to be a versatile element that can alloy with other elements, it is found that nickel is not a carbide former. Carbide formation, which is the second form of change mechanism in nickel alloys, is attributed to other elements alloyed with nickel that react with carbon making MC, M_6C, M_7C_3 and $M_{23}C_6$ carbides. $M_{23}C_6$ carbides form at the grain/twin boundaries and are considered to be the most influential in determining the mechanical properties of the alloys, but long time exposure at high temperature in the range of 760° to 980° C also causes precipitation of intra-granular carbides [4].

Precipitate particle size also influences the alloy's mechanical properties and it was noted that alloy hardness increases with particle size which is mainly governed by the heat treatment time and temperature. At creep temperature range applications (i.e. 60% melting temperature) these particles are susceptible to coarsening and that leads to a decrease in metal strength. This phenomenon is normally avoided by adding slow diffusion elements to the alloy like niobium and tantalum [4].These microsructural change mechanisms are believed to be effective in enhancing the alloy tensile strength property and not the cyclic loading strength.

As a matter of fact, it is expected that the evolution of precipitate particle due to aging treatment would actually cause deterioration in the alloy fatigue strength. This reduction in fatigue strength is believed to be caused by the material loss of ductility due to aging-induced carbide precipitation.

Welding of alloy 800HT is done frequently during new installation of equipment or maintenance work done in equipment such as reformer tubing welded joints with reformer pigtails or the latter welded with an outlet manifold piping system. Maintenance workshop welding is thought to be more critical, as it is done during rush periods like shutdowns of a petrochemical plant. In such circumstances, there exists high possibility of not having full control over the cleanliness of welded joints, the welding procedure and/or even the pre and post weld heat-treatment of the welded parts.

Such types of age-hardenable alloys are recommended to be pre-heated in order to reach an adequate state of metal formability required for welding, while annealing should be conducted for the reason of relieving residual stress introduced during the welding process [5].

During the welding process, improper heat treatment of austenitic steels containing 8 to 40% Ni, can lead to inter-granular corrosion. This occurs at temperatures between 425° and 760° C when chromium starts to deplete the areas surrounding grain boundaries and reacts with carbon (present as an alloying element) to produce chromium carbides. The

material is then said to be sensitized. Re-heating the material to a high temperature followed by fast cooling, stabilizing the material by adding niobium, tantalum, or titanium, and last by restricting carbon content in the alloy are methods to protect the alloy form inter-granular corrosion [4].

Precipitation-hardenenable iron-nickel-chromium alloys, in general, contain aluminum and titanium as strengthening elements. The higher the content of these alloying elements, the higher will be the strength of the alloy. The tendency of strain-aged cracking starts to be of a concern during welding as large amounts of Al+Ti are added to the alloy. In such cases, careful pre-weld and post-weld heat-treatments are essential in order to reduce that tendency of cracking [6].

The low content of Al+Ti in Alloy 800 provides good weldability characteristics. Alloy 800HT has the same weldability as alloy 800, and requires special welding electrodes suitable for the high creep-rupture application environment [2].

In general, three factors are thought to affect the fatigue strength of the welded joints [7], namely:

- The stress state in the load path through the weldment.
- The stress-concentration factor at the toe of the weld.
- The presence or absence of inclusions and other defects in the weld.

Cold working the welded joint increases the fatigue life as it inhibits the formation of cracks at the component surface, which is the normal site of fatigue crack initiation.

1.2 The present study:

As mentioned earlier, during service the alloy 800HT is exposed to high temperature environments and thus undergoes various thermal aging conditions. These in-service aging conditions bring about the formation of variety of complex precipitates at the grain boundaries as well as within the austenite grains. Such precipitates are believed to have a direct impact on the alloy mechanical properties and in specifically the fatigue strength. Despite the considerable amount of research conducted in this area during the past two decades, a proper identification of these precipitates and their role in altering the alloy fatigue strength behavior has not yet been illustrated. Thus, there exists a significant need to undertake a study which will provide a better understanding of the nature of these precipitates that are produced during the high temperature service conditions in the alloy structure and their role in altering the fatigue behavior of the alloy. Also the role of these thermally-induced carbides in determining the fatigue crack behavior needs to be clearly evaluated for this reason.

The objective of the present study is to obtain a proper understanding of the microstructural changes resulting from the high temperature exposure and its role in altering the fatigue behavior of the subject alloy. We intend to achieve this objective by pre-aging a series of fatigue test samples at various aging regimes followed by fatigue

testing under ambient laboratory conditions. In the absence of a high temperature fatigue testing apparatus, we believe that the effect of heat induced microstructural changes on the fatigue behavior of the alloy can be evaluated by fatigue testing the pre-aged samples. This will provide us with a better understanding of the precipitation behavior and its influence on the fatigue strength by avoiding the much more complex problem of elevated temperature fatigue testing.

The pre-aged specimens will undergo SEM microstructural examination in order to identify the thermally induced microstructural changes. Fatigue tests on the pre-aged samples will be carried out to evaluate the influence of these microstructural changes on the fatigue strength of the alloy. Fracture surface studies will also be conducted to determine the fracture surface morphology and the role of the precipitates in the fracture behavior. The details of the proposed work are outlined in chapter 3.0.

CHAPTER 2

LITERATURE REVIEW

2.1 The effects of temperature on 800HT Microstructure:

The microstructure of alloy 800HT is found to be very sensitive to material heat-treatment history [9-12]. Electro-discharge machining (EDM) analysis revealed that the primary coarse inclusions in the heat-treated samples of alloy 800HT are TiC carbides and the finer precipitates at the grain boundaries and within the grains to be $M_{23}C_6$ particles [12,13].

The solution treated samples revealed very low dislocation density except for randomly scattered coarse polyhedral Ti (C,N) particles in both inter- and intra-granular regions. These particles did not dissolve during the solid solution treatment[11,12]. These particles are considered as primary particles in the alloy metal matrix and show no rational orientation relationship with respect to the matrix structure. It is believed that these titanium carbide particles have first formed during the metal solidification process as nucleation sites and were able to resist any considerable change in shape, size, and distribution to subsequent heat-treatments and even high temperature cyclic deformations[12].

Other carbides like $M_{23}C_6$ are only found to start forming after high temperature exposure[11]. High concentration of carbide precipitates was noted near grain boundaries. It is believed that the higher dislocation density near the grain boundaries promote the formation of precipitates at these sites[13]. Carbide precipitates also tend to form at regions adjacent to the primary TiC carbide particles [12]. $M_{23}C_6$ carbide precipitates start forming at 650°C and were noted to complete formation at 1000 hours. The same trend of carbide formation was also reported at 760°C. An internal stress has been suggested to exist, around these carbide particles, which acts positively in reducing the movement of dislocation and hence reducing creep rate. Theoretical expressions for such stresses cannot easily be derived due to the complexity of the actual loading situation [9].

The formation of $M_{23}C_6$ carbide precipitates were reported to cause the reduction in ductility for Alloy 800HT, which in turn leads to a reduction in the material fatigue strength[12]. In fact, a ductility exhaustion model was introduced to estimate the material fatigue life based on the material ductility reduction due to exposure to high temperature[8].

$M_{23}C_6$ precipitation at grain boundaries makes the alloy subject to inter-granular corrosion in oxidizing environments. This occurs due to the sharp decrease of chromium content adjacent to these particles[12]. The microstructure of 650°C and 760°C heat-treated samples was also found to be essentially identical for similar aging times. With higher carbon content of 0.8%, the grain boundaries carbide network structure coarsens and carbide particles start to precipitate inside the grains during heat-treatments at 870° and

980°C. No such effect is found for the lower carbon content of 0.4% at these high temperatures, and the microstructure remains the same at the lower temperature treatments. It was also reported that TiC precipitation occurs readily at 900°C temperature environment, while at 800°C, $M_{23}C_6$ particles precipitate preferentially[14]. At 850°C heat-treatment, similar precipitation was noted for both particles. At 750°C, the $M_{23}C_6$ precipitation was particularly clear and high concentration of these particles was found associated with dislocation and dislocation tangles in the intra-granular regions. Grain boundaries, at this treatment, also contained discrete $M_{23}C_6$ particles as well [9].

Carbide particle precipitation was noted [9] to form coarser and fewer particles when stress effect is added to the test environment as compared to the stress free testing conditions outlined earlier. Such change in precipitation behavior of the material clearly outlines the creep effect on the rate of particle coarsening rate. The effect of material pre-aging treatment has been studied [9] with the purpose of determining its effect on subsequent material resistance when subjected to creep environment. It has been noted that the initial creep strength of water quenched annealed 800HT components has improved due to the increase in dislocation density which in turn has lead to uniformly scattered fine carbides and stable dislocation structure. Unfortunately these fine particles are found to coarsen with time and therefore lose their ability to resist creep damage, hence after a period of exposure to high temperature environment the material tends to lose the positive effect on creep strength of initial heat-treatment.

2.2 The effect of aging on the fatigue strength of alloy 800HT:

While pre-aging of alloy 800HT has provided some initial creep strength improvement that diminished with time, the material fatigue strength has shown a different trend with different heat-treatment histories. Improved fatigue life was shown to result for material subjected to aging treatments at 550°C[11]. With this under aging material condition, particle shearing is thought to be an important strengthening mechanism along with the positive effect of reduced stage I crack growth rate due to precipitate shearing resulting in highly reversible plastic flow.

At higher test temperatures, considerable deterioration in fatigue strength was observed. This is noted to be combined with a change in the material carbide precipitation behavior under microscopic examination. The material experiences the formation of various types of precipitates as it undergoes high temperature fatigue testing. Precipitates like $M_{23}C_6$ and TiC particles form with clear dependency between the test temperature/strain rate combination with the particle size, shape and location[11].

Dislocation density was also observed to increase more rapidly during high temperature fatigue testing as compared to the stress free heat-treated samples. A large number of dislocation pairs are noted to form at a strain rate of $5X10^{-3}$ S^{-1} at 600°C. These dislocation pairs provide preferred nucleation sites for the $M_{23}C_6$ particles[13]. These dislocations are found to be arranged in planar arrays and, due to their interaction with

$M_{23}C_6$ carbide particles at the grain boundaries. they have a major effect of inhibiting grain boundary migration[11].

As one goes higher in testing temperature. to 750°Cand 850°C, fatigue damage start to set in with the formation of parallel plates of $M_{23}C_6$ at the grain boundaries and twin boundaries[12]. At a fatigue testing temperature of 850°C and a strain rate of $4x10^{-4}$ S^{-1}. large amounts of very fine cube-shaped $M_{23}C_6$ particles are observed in the matrix. These particles are thought to serve as pining points for moving dislocations [12]. At this high temperature, large amount of secondary TiC particles along with $M_{23}C_6$ precipitates are found both inter- and intra-granularly, with the TiC particles preferring intersecting dislocation regions for precipitation [12]. At 950° C, TiC carbides were found [12] to be predominant and co-existent with $M_{23}C_6$ again at both inter- and intra-granular regions.

As with the fatigue strain rates. tests have also shown a direct relationship with particle precipitation and hence the fatigue life. Decreasing strain rates were noted to lead to coarsening of inter-granular $M_{23}C_6$ particles and the formation of a continuous layer of $M_{23}C_6$ on some of the grain boundaries [12]. The total volume fraction of inter-granular precipitates significantly decreased and their size increased with higher temperatures and lower strain rates.

Fatigue damage mechanisms were studied for alloy 800H when subjected to cyclic strain testing at high temperatures. The damage evolution was claimed to be successfully

predicted as a function of plastic strain range. At $5X10^{-3}$ S^{-1} strain rate and at 600^{0} C testing temperature alloy 800H experienced cyclic hardening, as compared to A 316 stainless steel that showed cyclic saturation in similar environments [11].

The effect of both circumferential and axial defects in alloy 800H tubular components have drawn interests of researchers to simulate as close as possible actual plant loading conditions for this widely used alloy as a heat exchanger component in the power and petrochemical industries[13]. These studies have covered the cyclic loading effects as well as steady state creep deterioration, where initiation and growth of creep cracks can be life limiting.

Tensile hold time is thought to effect deterioration of fatigue resistance through initiation, growth and linkage of grain boundary cavities, and subsequent inter-granular crack propagation [8]. On the other hand, trans-granular crack propagation is observed in the conditions of only compressive, or with equal compressive and tensile hold times. Primary and secondary side cracking of tubes was noticed in loaded components at nuclear steam generation applications [15].

Several production lots, semi-finished material, and welded components have been tested at the sites of different companies, namely ABB, Siemens-KWU and KFA for alloy 800 and alloy 617 using different techniques[16]. This was done in order to eliminate the influence of uncontrollable testing parameters and to come up with a wider database for

these alloys. Materials that were in service for 8000 hours at temperatures between 600° to 900° C were tested and their results were compared with results from tests for unexposed materials to evaluate the creep and fatigue crack growth behavior for the two alloys under both conditions.

Results show the Fatigue Crack Growth (FCG) to be well described by the linear parameter ΔK, while Creep Crack Growth (CCG) was well described by the energy rate integral C^*. It is also worth noting that most of the experiments on CCG have been performed with testing times up to 2000 hours, while the service times of real components are much longer. Thus the admissibility of the extrapolation has not been proven yet for such applications. In addition to this, the actual loading conditions were usually much more complicated as compared to the simple uni-axial loading conditions used in these tests[16].

In general, the fatigue loading enables the nucleation and growth of carbides to proceed quickly due to the generation of nucleation sites such as dislocation and dislocation tangles. The low cycle fatigue life decreased with increasing temperature and decreasing strain rate due to the transition in crack initiation and propagation mode from trans-granular to inter-granular. This reduction in Low Cycle Fatigue (LCF) life resulted from homogenization of slip and an accompanying increase in inelastic strain generated in a fatigue cycle and partly from inter-granular crack initiation resulting from oxidation of surface-connected grain boundaries and rapid propagation through embrittled grain

boundaries[12]. This may support the observation that crack initiation has always occurred at the specimen surface accompanied with the formation of intrusion and extrusions while crack propagation was almost always trans-granular[11].

2.3 Fatigue failure mechanism of alloy 800HT:

K Bhanu et. al.[10] have studied the fatigue failure mechanism of alloy 800H at high temperatures and under various cyclic loading rates of tension and compression. It was observed that the fracture mechanism was governed by the tension loading rates, where fast tensile loading rates resulted in trans-granular cracking behavior in the initiation as well as the propagation stages of fatigue life. Slow rates ($4X10^{-5}$ S^{-1}) of cyclic loading, on the other hand, resulted in inter-granular crack initiation and propagation.

Cavity formation observed during Low Cycle Fatigue asymmetrical cyclic loading tests, where loading and unloading occurs at different rates, led to shorter cyclic lifetime. Such phenomenon was not noted in the case of symmetrical loading tests. Nucleation and growth of cavities were noted to take place during fast compression and slow tensile half tests. Z. Mu et. al. utilized experimental data and presented a physical model that has claimed a LCF life for alloy 800H. In this model, it was assumed that the main fatigue life-limiting factor to be the growth of fatigue cracks. Plastic deformation, creep and cavity-crack interaction were considered to be contributing to the crack growth[14].

A smaller plastic strain component and a reduced stage I crack propagation rate for the alloy 800H have both contributed to longer fatigue life. Alloy 800H had experienced localized slip due to the shearing of small gamma prime particles as compared to A316, which had dislocation cells forming at all strain ranges.

The two alloys were noted to have accumulated damage in a similar manner even though their deformation behavior differs [17]. With regard to the crack propagation mode, it was noted that cracks were predominantly trans-granular under fatigue condition, while cavity processes controlled creep and hold time conditions. [1]

For alloy 800H, the tensile hold period during cyclic loading was noticed to cause inter-granular cracking. At 1.0 % strain range, tensile hold loads at 650°C were more damaging than compressive loads. However, for the compressive hold period testing performed at 0.4% strain the inverse was found to be true. At 760°C, the tensile hold periods appeared to be consistently most damaging and fatigue life was reduced with increasing hold period [8].

High temperature time-dependent fatigue, i.e. creep fatigue interaction, is normally caused by creep damage, corrosion fatigue, mean stress, micro-structural instabilities, and irradation damage, all of which are found to be mostly time and possibly wave form dependant[8].

Interaction of fatigue and creep condition, for alloy 800H, had attracted a decent amount of attention since it resembled actual life loading conditions seen in process plants. Various strain rates and waveforms were applied by different researchers in an effort to simulate plant start-up and shutdown heating and cooling conditions. The combined effect of creep, fatigue and oxidation has seriously affected low cycle fatigue (LCF) life under hold time conditions at 850°C [10].

The creep behavior of alloy 800HT was examined over the temperature range of 700°C to 900°C of stress ranging from 30-170 Mpa. It was found that the, solution treated and quenched test specimens gave longer creep life than over aged test samples. This difference in creep life increased at lower creep stresses for a given test temperature. Precipitation of $M_{23}C_6$ carbides are thought to be behind such phenomenon during the early stages of creep by introducing internal stresses that ratcheted moving dislocations [9].

C P Hunter et. al. [13] have also studied the creep crack growth (CCG) behavior of alloy 800H on circumferentially notched tube samples at 800°C using the DC potential drop method. It was shown that the C* integral is an appropriate parameter for describing this behavior. They have also demonstrated good agreement between component test and conventional (compact tension specimen) CCG data. This study, made by CP Hunter [13], has also resulted in the development of a method describing the CCG deterioration rate of alloy 800H and showing that the use of the C* integral leads to a satisfactory correlation between conventional and notched tube test specimens. Internal pressure loading was

shown to develop a significant degree of weakening as compared to tensile loading. It was also shown that the crack propagation behavior changed from trans-granular to inter-granular [14]. This demonstrates fatigue creep interaction.

Formation of internal damage has been attributed to creep deformation during the tensile loading of fatigue cycles. The compressive part of the cycle was also demonstrated to be an important part in cavity nucleation.

2.4 Oxidation effect:

It is proposed that, of all time dependent deterioration processes, oxidation processes were noted to have the largest impact on the fatigue and creep life of the alloy [10,18]. It was also observed that deformation ratcheting had its greatest influence on the alloy fatigue life during the asymmetrical cyclic loading conditions.[10]

During the fast tensile/fast compression fatigue loading condition [10] spallation of surface oxide scales was observed, and this lead to the development of very rough surfaces. Metallographic observation of fatigue samples has revealed that micro-cracks initiate at surface grain boundaries within the thin oxide layer[12]. Chromium is found to deplete in the initial stages of fatigue testing at the sub-surface regions.

During this stage, rapid oxide scale growth occurs which removes the chromium from the subsurface region out towards the oxidized sample surface. This phenomenon makes the

area less protective and prevents the healing of oxide scale cracks, which leads to an increase in internal oxidation along the grain boundaries and in turn causes the formation of surface cracks[12].

Crack propagation is believed to be promoted by the oxidation at the inter-granular crack tip and by the presence of cavities that lead to the formation of a thin layer of brittle material. Cavities are also noted to start nucleating from CO and CO_2 gas bubbles caused by oxygen reacting with grain boundary particles. This oxidation process depends obviously on the alloy temperature and the presence of oxygen. The matrix mismatch at the grain boundaries forms an easy oxygen path and is believed to be the reason for the high rate of oxidation at these sites. The presence of Cr and Ti elements in the form of carbides, at the grain boundaries also promotes such oxidation process [12]. Crack tips are observed [10] to have an oxidized appearance that suggests that the oxidation process continues during the crack growth stage.

For un-aged samples, crack tip oxidation, which causes an accelerated crack propagation rate, along with the formation of porosity beneath the oxide scale, that acts as crack nucleation sites, are reported to be two major environmental factors affecting the alloy high temperature fatigue strength. However, the formation of tensile stresses at the specimen surface, due to general oxidation, and grain boundary weakening, due to inter-granular oxidation of titanium and aluminum, are considered to be less detrimental[18].

Pre-oxidation time (i.e. pre-aging in air) is reported to play an important role in the crack initiation process. After 100 hours of pre-oxidation at 800° C the alloy was found to experience surface cracks after two fatigue deformation cycles, while with 400 hours of pre-oxidation, surface cracks were only reported [12] after a few hundred deformation cycles. This behavior is proposed to be governed by the changes to the oxide layer.

2.5 The Effect of Aging on Fatigue Strength of Welded Joints:

None of the sited technical references on alloy 800 series has addressed the effect of aging on the alloy weldment. However, such work has been conducted on weldmens made of other alloys like 304, 308 stainless steels as well as alloy 718 nickel base super alloy.

K. Bhanu et. al. have conducted their high temperature fatigue testing at 823 and 923 K on type 304 stainless steel (SS) material, type 308 SS weld metal and 304-308 SS weldmens prepared by manual metal arc welding process[19]. Their test results indicated that the low cycle fatigue resistance of base material was superior to that of the weldment at both test temperatures. Also, a reduction in fatigue life was noticed when the test temperature was raised from 823 to 923 K. It was observed that the δ-ferrite in the weldment has transformed to $M_{23}C_6$ and σ phase during fatigue testing[19].

Wakia et.al. have conducted their fatigue testing at 923 K on friction welded joints made of type 304 SS and alloy 718 Nickel based super-alloy. Their fatigue test results indicated

that the 304 welded specimen has inferior fatigue strength in comparison with the base metal. However, alloy 718 specimens exhibited fatigue strength equivalent to that of the base metal. The cyclic softening and large yield stress were the main cause of the large fatigue life of the welded specimens[20].

CHAPTER 3

EXPERIMENTAL WORK

The objective of this study was realized through pre-aging a series of fatigue samples at 3 different temperatures and at four different time periods. These pre-aging temperature/time regimes are provided in table 1. These pre-aged samples were fatigue-tested under ambient laboratory environment to examine the influence of the aging treatments on the fatigue strength of the alloy. The fatigue fractured specimens were also examined using SEM in order determine the effect of aging on the microstructure of the alloy and the relationship of these changes on the fatigue crack initiation and/or growth mechanism and the effect on the material fatigue strength. The detailed outline of the proposed work is as follows.

3.1 Material and specimen geometry

The material used in this study was a commercial Incolloy alloy 800HT, which is an austenitic iron-based wrought super-alloy. This alloy contains high composition of nickel and chrome. It was received in the form of 3-mm thick hot rolled sheets in an annealed condition. The annealing was carried out at 1200° C for 10 minutes followed by air-cooling. This annealing resulted in an average grain size of ASTM 3.0. The material microstructure in the as received condition contained titanium carbides and titanium

nitrides located inside the grain structure. These small angular inclusions are readily visible in the un-etched state and vary in color from the orange-yellow of the nitrides to the gray-lavender tint of the carbides. These particles are formed during the metal solidification stage and remain to be very stable in subsequent heat-treatments. Chromium carbides start precipitating only after high temperature exposure between 540° and 1095° C, and they result in sensitization of the alloy. The vendor certified chemical composition of the test material and the alloy's mechanical properties are listed in tables 2 and 3 respectively. Figure 1 shows the hourglass fatigue test specimen geometry to be used to generate the fatigue data. The fatigue specimens were machined from the 3-mm thick sheets such that the long axis of the specimens coincided with the direction of the rolling.

Welded specimens were also used in this study. 3mm thick sheets of alloy 800HT were joined by Gas Tungsten Arc Welding (GTAW) technique in an industrial welding shop, and then machined to properly sized fatigue test specimens with the weldment being in the middle of the specimen (figure 2). The welding was conducted by a day-to-day shop welder performing the routine welding activities in one of the petrochemical plants. A single GTAW pass was made first after sheet joint preparation and set-up on one side of the joint, with the other side subjected to normal atmospheric environment. As a result, porosity is expected to form in the sheet joints at the back side, and should be mechanically grinded off removing any porous material until reaching the solid weld metal. This was followed by another single welding pass on the backside to compensate for the incomplete penetration of the first pass. The plant actual component welding

procedure asks for Inconel 625 as filler metal with 2.4 mm electrode size, with no pre-weld or post-weld heat treatments required, but it is required to have inert gas (argon 99.9%) flowing with 9 to 11 liters per minute inside the tubular component that is being welded. This is designed to protect the component inner side from oxidized porosity. These samples were subjected to heat treatment and fatigue testing similar to that done to the regular samples. This will allow for the evaluation of the weldment fatigue properties as compared to the regular specimens.

Regular and welded fatigue samples were then subjected to the aging treatment regimes outlined in table 1. All aging treatments were conducted in an air environment. Similarly, SEM microstructural test specimens were aged under the same aging regimes for conducting SEM examination.

3.2 Mechanical Testing

The fatigue testing was carried out using an Instron 8501 material test system, available at the KFUPM Advanced Materials Laboratory. Instron 8501 is a closed-loop servo-hydraulic, dynamic, mechanical testing machine that is capable of generating various constant and alternating tensile and compressive stress amplitude loading to test specimens. This fatigue loading can be position controlled (+/-75 mm), stress controlled (+/- 100 KN), or strain controlled, with a frequency range of 0 to 200Hz.

Fatigue testing of the material was carried out, under ambient laboratory condition, for the as-received solution-treated annealed fatigue samples as well as for the heat-treated fatigue specimens. The fatigue testing in this study was done at 20 Hz loading frequency and with fatigue loading ratio $R=0.1$. This task is to provide basic fatigue data in order to evaluate the effect of such heat-treatments on the material fatigue strength. The cyclic testing was under load control condition to generate the fatigue data with life range of 10^3 to 10^6 fatigue cycles.

3.3 Microstructural characterization

The alloy microstructure changes resulting from the materials various aging treatments was analyzed with the help of Scanning Electron Microscopy (SEM). The Joel JSM T-300 Scanning Electron Microscope, equipped with an energy dispersive spectroscopy (EDS) system, was utilized to perform spot analysis to identify the type of inter-granular and intra-granular precipitate particles. Fractured surface morphology examination was also performed, by SEM, for most fractured fatigue test specimens. This fractographic examination work has revealed the direct relationship between fatigue crack behavior with the specimen microstructure resulting from the specimen aging history and the effect on the specimen fatigue strength. This was aimed to lead to an understanding of the role of the intra-granular, the inter-granular as well as the twin boundary precipitates in controlling the fatigue cracking behavior and hence the specimen fatigue strength.

CHAPTER 4

RESULTS

4.1 The Effect of Aging Temperature on Fatigue Strength:

The data collected from the fatigue testing of alloy 800HT are summarized in tables 4 to 9. These fatigue test results were grouped into four sets of data, each representing the effect of the aging temperature at a fixed time period of specimen thermal aging heat treatment. These four sets of data were then plotted as figures 3, 4, 5 and 6. Fatigue data for the as-annealed specimen were also plotted in all four figures for comparison reasons.

At 24-hour aging time, figure 3, one can clearly observe that the aging temperature curves show lower fatigue strength than the as-annealed data curve. These three temperature curves look somewhat congested suggesting no effect, but with a closer look we notice a decrease in fatigue strength with increasing aging temperature.

The as-annealed specimen fatigue data is still showing improved life compared to other aged specimen for the 100 and 500 hour aging time conditions (figures 4 and 5 respectively), with the same trend of decreasing fatigue strength with increasing aging temperature. The 100-hour aging temperature curves (figure 4) start to develop a noticeable reduction of fatigue strength with increasing pre-aging temperature. However, at 500 hour aging time figure 5 shows that the aging temperature curves are positioned in

a very clear manner that strongly supports the earlier mentioned aging temperature effect on fatigue strength.

Figure 6 represents the aging temperature effect at 1000 hour of aging time. The figure shows a large reduction in fatigue life as a result of aging at 870°C. Surprisingly however, the fatigue data for aging at 650°C for 1000 does not indicate any appreciable degradation in the fatigue strength of the alloy. In fact, the data for the 650°C aging for 1000 hours coincides with data for the as received condition.

From all three figures, presented, we can gather that aged alloy 800HT specimens have experienced lower fatigue strength than the as-annealed samples. We can also state that, for alloy 800HT, the aging temperature directly affects fatigue life and that increasing the pre-aging temperature for the alloy generally leads to a reduction in specimen fatigue life, and that this trend is better observed at higher aging temperatures. The alloy in the as-received condition has undergone an annealing treatment, which improves the specimen fatigue life, and this can be observed in figure 7 as compared to the solution treated specimen.

4.2 The Effect of Aging Time on Fatigue Strength:

The same fatigue data for 800HT were then regrouped in three sets of data each outlining the effect of aging time at a specific aging temperature condition. Figures 8,9 and 10 show the S-N time curves (24,100, 500 and 1000 Hour.) for the three aging temperature

conditions 650°, 760° and 870°C respectively. The aged specimens are noted to be generally lower in fatigue strength than as-annealed specimens, in the three tested aging temperature conditions. At 650°C aging temperature, figure 8, the 24-hour aging time curve gave the lowest fatigue strength, lower than the as-received curve. The other two aging times, namely 100 and 500 hours, gave smaller fatigue strength reductions. The 1000-hour aging temperature at 650° C, however, exhibits fatigue strength similar to that of the as-annealed specimens.

Similarly, the fatigue test data for the specimens aged at 760°C (figure 9) has shown lowest fatigue strength for the 24-hour aging time as compared to the specimens aged for 100 and 500 hours. All these specimens still exhibit lower fatigue strength than that of the as received. However, for the 870°C aging temperature (figure 10) results do not show a similar trend for the 24 hour aging treatment. A similar observation can be made for the effect of aging at 870°C for 500 hours.

In general, we can state that the aging time effect is not consistent at all aging temperature ranges, and that the as-annealed curve generally gave higher fatigue strength when compared to the aging time curves. At low aging temperatures, it is noted that the lowest aging time offered lowest fatigue strength, while at high pre-aging temperatures, the highest aging time gave the lowest fatigue strength.

4.3 Microstructural Characterization:

SEM examination done to samples of the various aging conditions was thoroughly conducted to analyze the microstructural evolution of alloy 800HT that is brought about by aging treatment times and temperatures and to observe how such changes in specimen microstructure tend to affect the alloy fatigue strength. Previous EDS analysis has identified carbides evolving during the aging heat-treatment process to be fine inter-granular and intra-granular $M_{23}C_6$, and primary coarse TiC inclusions[12,13]. EDS spot analysis was also used in this study to determine the type of precipitate carbides present inside the grain structure and at the grain/twin boundaries, figures 11 and 12 respectively.

Specimen aged at 650°C for 24 hours was observed to have no noticeable carbide precipitates at the grain boundary, twin boundary or within grain matrix (figure 13). Spot analysis indicates the precipitates to be $M_{23}C_6$ as previously reported[9,10]. However, TiC carbide primary particles were noted to be randomly distributed within the grains. Similar comments can also be made with regard to the specimen aged at 760°C for 24 hours where small amounts of precipitates were observed at the grain boundaries and also within the grains. Aging at 870°C for the same aging time of 24 hours, produced significant amounts of carbide precipitates at grain boundaries, twin boundaries and within grains (figure 14). A fine continuous network of grain boundary precipitates has developed at this aging condition. The precipitates at the twin boundary are observed to be discontinuous.

Aging at 650°C for 100 hour brought small amounts of fine particles within the grain matrix and at the grain boundaries (figure 15). TiC particles were observed at grain boundaries and in the matrix while no noticeable twin boundary precipitates were observed. Specimen aged for the same time period at 760°C shows a fine network of carbide precipitation at grain boundaries, twin boundaries, and appreciable amounts of grain matrix precipitates (figure 16). This phenomenon became more visible in the microstructure of specimen aged at 870°C for 100 hours (figures 17 and 18), where we notice carbide precipitation at the grain boundary and twin boundary regions along with large amounts of intra-granular carbide precipitates.

Specimens aged for 500 hours shows continuous network of $M_{23}C_6$ precipitates at the grain boundary at all three aging temperatures. Aging at 650°C did not result in the formation of precipitates at twin boundaries (figure 19). However, aging at 760° and 870°C has produced coarse and continuous precipitates at the twin boundaries (figure 20). Only very small amounts of precipitates are observed within the grain for the 650°C sample. These precipitates are noted to be increasing in quantity with increasing aging temperature.

Specimen aged at 650°C for 1000 hour was observed to have a fine and continuous network of carbide precipitates at the grain boundaries (figures 21 and 22). Precipitates at the twin boundary were discontinuous, while small amounts of precipitates were observed within grain matrix. A continuous heavy and extensive coarse carbide particle

precipitates were observed at grain boundaries of specimen aged for 1000 hours at 870°C (figures 23-26). The twin boundary precipitates, at this aging condition, were noted to be fine and continuous, while the TiC and $M_{23}C_6$ particles showed more presence at the grain structure as well as at the grain boundaries.

4.4 Fracture surface study:

Fractured surface examination was performed using SEM in order to study the fatigue crack morphology for alloy 800HT specimen with various aging heat treatments and how this all affected the specimens fatigue strength. Fatigue cracks, in all variously aged specimens, were observed to be initiating mostly at the specimen surface, with occasional crack initiation at sub-surface sites. The crack morphology has revealed three main regions, namely crack initiation, propagation and overload regions. In nearly all cases, cracks initiated at the specimen surface and propagated independently coalescing to form major cracks that propagated through the specimen width before reaching the overload zone where the final separation occurred. Soo and Sabatini[20] reported a similar phenomenon.

The crack initiation mode was mostly trans-granular with some exceptions as in the case of specimen aged for 500 hours at 760° and 870° C. In the latter two cases, both inter-granular and trans-granular crack initiation modes were observed. The crack propagation was generally trans-granular in all the specimens examined irrespective of their aging condition.

The crack initiation regions were characterized to be mainly flat with river patterns near crack initiation sites (figures 27-29). The crack propagation regions were observed to be relatively rough having finely spaced fatigue striations (figures 30-32) along with varying amounts of secondary cracking (figures 33-36). An increase in size and density of these secondary cracks were observed to coincide with increases specimen aging time for all four aging time conditions. The most sever secondary cracking occurred in the 870°C samples aged for 1000 hours (figure 36). Figures 37 and 38 show a general view of the fracture surface morphologies for the specimens aged at 870°C for a period of 24 hours and 100 hours respectively.

4.5 The Effect of Aging Temperature on the Fatigue Strength of Welded specimens:

The fatigue data of the welded specimens are presented in table 9. The fatigue test results for the as-received welded specimens as well as for welded specimens aged at 650°C, 760°C and 870°C are plotted in figures 48-52. The aged specimens have, generally, given lower fatigue strength as compared to the as-received specimens (figure 48). This is found to be consistent with the fatigue data of regular un-welded specimens, as described earlier. Further to this, figures 49-52 represent a comparison between regular un-welded specimens and specimens welded for 100 hours at 650°C, 760°C and 870°C. All four figures show that the welded specimens exhibit reduced fatigue strengths when compared to regular un-welded specimens.

CHAPTER 5

DISCUSSION

5.1 General:

The results of the present study indicate that the fatigue strength of alloy 800HT is generally sensitive to the material thermal aging treatment. The aging treatment was observed to produce significant changes in the material microstructure in the form of various precipitates that are formed at the grain boundaries, twin boundaries and at the grain matrix. Due to these microstructural changes, the aging treatment therefor is expected to affect the mechanical properties of the alloy including the material Fatigue Strength.

When subjected to fatigue loading the alloy fatigue resistance was noted to be affected by the material thermal aging history. In this study, the effect of aging on the fatigue resistance of the alloy is explained by examining the role of the microstructural features in inducing the changes in the crack initiation and crack growth behavior of the alloy. This phenomenon is best explained by examining the fatigue crack behavior of the alloy as influenced by the changes in the material microstructure resulting from the various aging treatments

The three aging temperatures, namely 650°C (1200° F), 760°C (1400° F), and 870°C (1600° F), were selected to represent the range of service temperatures that the Alloy 800HT is expected to be exposed to during service in typical applications in petrochemical process industries. A number of studies have been undertaken during the last few years to examine the effect of exposure of alloy 800HT to the above mentioned temperatures. As mentioned earlier, one such study reports that after 1000 hour of aging, the microstructure of alloy 800HT reaches a fairly stable state with regards to the preciptate formation[9]. This stabalization is believed to be caused by the depletion of carbon, which is needed for the carbide formation. However, since the formation of carbide precipitates are known to start quite early, aging time periods of 24, 100, 500 and 1000 hours were selected to explore the gradual effect of aging on the alloy microstructure and hence the effect on the fatigue strength within the 24 hours to 1000 hours aging time.

5.2 The Effect of Aging on Fatigue strength at 24 hours aging time:

For the 24-hour aging treatment, the fatigue strength is found to decrease for the specimen aged at all the three selected aging temperatures, namely 650, 760, and 870°C, as compared to specimens in the as-received condition (figure 3). It is also clear from this figure that the fatigue strength of the alloy decreases with increasing the aging temperature. The microstructure of the specimens aged for 24-hours was observed to contain varying amounts of $M_{23}C_6$ carbide precipitates depending on the aging temperature. Specimens aged at 650°C contained only a very small amounts of

discontinuous grain boundary precipitates (figure 13), and exhibit slightly higher fatigue strength relative to specimens aged at 760°C. An examination of the microstructure reveals that at 760°C the 24 hour aging result in the formation of small amounts of precipitates within the grain matrix. A relatively larger amount of precipitates are observed at the grain boundaries, grain matrix and some twin boundaries in the specimen aged at 870°C (figure 14). These specimens exhibit a further reduction in the fatigue strength (figure 3).

The observed reduction in the fatigue strength of alloy 800HT due to the aging for 24 hours prior to fatigue testing can be attributed to the role of various carbide precipitates in enhancing the fatigue crack growth. The examination of the fractured surfaces of a specimen aged at 650°C reveal a very flat brittle fracture surface showing no considerable secondary cracking (figures 27 and 39). The fracture surface morphology suggests a trans-granular mode of fracture in the crack initiation and propagation regions. These brittle carbide particles could have contributed in causing an early initiation of the fatigue cracks and enhancing the fatigue crack growth rate as compared to the un-aged specimens.

The fractured surface of the specimen aged at 760°C show a fairly flat and brittle surface with a relatively larger amount of secondary cracking in the crack propagation region (figure 40). As mentioned earlier, the specimen aged at 760°C contains a relatively larger amount of precipitates at the grain boundary, twin boundary and matrix regions as

compared to the specimens aged at 650°C. The larger amounts of secondary cracks found in the fractured surfaces of the specimen aged at 760° C could be associated with the presence of the brittle carbide precipitates. Greater amount of extensive secondary cracks are noted in the 870°C fractured surface (figure 33) and can be attributed to the larger amounts of grain matrix and twin boundary precipitates revealed by SEM examination of these aged specimens. These precipitates have lead to a relatively rougher crack surface for the 870°C samples (figure 37) as compared to lower temperature fatigue samples.

5.3 The Effect of Aging on Fatigue strength at 100 hours aging time:

The fatigue examination of the fatigue test results for specimens aged for 100 hours, again, show a clear reduction of fatigue strength with increasing aging temperature (figure 4). This reduction is observed to be more noticeable as compared to the specimens aged for 24 hours. Here, we also see that the formation of carbide precipitates, due to aging, plays a major role in governing the fatigue crack morphology and, in turn, determining the alloy fatigue strength.

The relatively higher fatigue strength for the 650°C samples can be attributed to lower amounts of secondary cracking (figure 41) when compared to specimens aged at higher temperatures. This is due largely to the presence of lower amounts of grain matrix and twin boundary carbide precipitates (figure 15). However, the 760°C specimens contained relatively more grain matrix precipitates and have also started to show discontinuous network of grain boundary precipitates (figure 16). Therefore, this can explain the

observed relatively rougher fractured surfaces and the higher amounts of fatigue secondary cracking (figures 34, 42) that causes the reduction in fatigue strength. More of the grain matrix and twin boundary carbide precipitates are noted form in the 870°C specimens (figures 17 and 18) with semi-continuous twin boundary network of precipitates and has resulted to induce a larger amounts of secondary cracking (figure 31) and further reduction in fatigue strength.

The fatigue crack morphology, of these 100-hour aged fractured samples, also suggested a trans-granular mode of fracture, in the crack propagation and initiation regions, for all aging temperatures. The fractured surfaces at this aging time appear to be rougher and have larger amounts of secondary cracking for specimens aged at higher aging temperature. This phenomenon is believed to directly affect the fatigue strength of the alloy and can be attributed to the amounts of precipitates formed at the grain matrix and twin boundaries.

5.4The Effect of Aging on Fatigue strength at 500 and 1000 hours aging time:

Specimen aged for 500 and 1000 hours are also observed to have similar fatigue behavior. Higher temperatures have generally lead to the formation of more grain matrix and twin boundary precipitates and are observed to cause the triggering of more secondary cracking and, as a result, more reduction in fatigue strength. The grain boundary precipitates are generally observed to be increasing with higher aging

temperatures, but with no noticeable effect in the fatigue strength. This can be noticed for these two aging time periods but more clearly with the specimens aged for 1000 hours.

Samples aged at 650°C, for 500 hour, have a relatively higher fatigue strength (figure 5) and are observed to have less twin boundary and matrix precipitates (figure 19), but show similar amounts of grain boundary precipitates as compared to samples aged at 870°C for the same aging period (figure 20). The crack morphology of the 870°C fractured samples (figure 35 and 43) clearly reveal extensive secondary cracks that are attributed to the large amounts of matrix and twin boundary precipitates.

For the 1000 hour aged specimens, the phenomenon becomes more obvious. SEM examination of samples aged at 650°C show fine grain boundary network of precipitates with discontinuous twin boundary network of particles and small amounts of intra-granular precipitates (figure 21, 22). This is reflected in the flat trans-granular crack initiation and propagation regions and in the observed reduced number of secondary cracking at these regions (figure 44).

On the other hand, samples aged for 1000 hours at 870°C have shown coarse network of precipitates at the grain boundary regions with semi-continuous network of fine particles at the twin boundary regions. This was accompanied with increased amounts intragranular $M_{23}C_6$ and TiC particles (figures 23- 26). Fractured samples having this aging treatment have indicated rougher crack initiation and propagation regions with

extensive secondary cracking, figure 36. This all explains very clearly the reported reduction of fatigue strength (figure 6).

It is however surprising to note that the specimen aged at 650°C for 1000 hours did not show any fatigue strength reduction when compared to the as-received material. An examination of the microstructure indicates a reasonable amount of carbide precipitation at the grain boundary regions and small amounts of carbide precipitation within the grains (figures 21 and 22). The fracture surface study (figure 44) does not exhibit a significant amount of secondary cracking. No reasonable explanation was found for this surprising fatigue results for the specimens aged at 650°C for 1000 hours. Further investigation of this phenomenon could be undertaken by future work.

The fact that the fatigue cracks were generally trans-granular in the crack initiation and propagation regions supports our argument which suggests that the aged specimens were generally not weakened due the formation of grain boundary precipitates. During fatigue testing, precipitates formed within the matrix grains and at twin boundaries are noticed to help the fatigue trans-granular crack to propagate faster through the specimen leading to reduced fatigue strength.

The formation of intragranular $M_{23}C_6$ precipitates has been reported to produce a relatively more brittle alloy structure[12]. Higher aging temperature has lead to more $M_{23}C_6$ particles precipitation inside the alloy matrix and therefore reduce the material ductility

which can explain the reduction in the material fatigue strength. Inter-granular carbides are also considered to introduce localized high stress areas inside the alloy matrix. These sites are believed to promote the formation of primary as well as secondary cracking during the fatigue loading which weakens the alloy matrix and makes it easier for the crack to propagate through leading to lower fatigue strength.

Higher aging temperature is also believed to produce a thicker oxide layer at the surface of the aged fatigue specimen. This brittle oxide layer is believed to be increasing with increasing aging temperature and is reported to promote the fatigue crack initiation process which leads to the weakening of the specimen fatigue strength. General oxidation at the surface of the aged specimen is enhanced by increasing aging temperature, and lead to the formation of surface tensile stress. This phenomena is also considered to be a factor in reducing the aged specimen fatigue strength. However, this factor is considered to be less detrimental[18].

The effect of aging temperature on the fatigue strength of alloy 800HT can be further outlined in figures 45-47. It is clear from these figures that increasing the aging temperature leads to a general reduction in the alloy fatigue strength. This trend has proven to be consistent at all three fatigue life regions, namely low, mid and high cycle at 5,000, 50,000 and 2,000,000 N_f respectively. It is also evident from all three graphs that the aging time was not as effective in reducing the alloy fatigue strength in all three fatigue life regions.

5.5 Fatigue Strength of Welded Specimens:

The fatigue testing conducted on the aged welded fatigue specimens clearly outline the effect of the aging treatment on the alloy fatigue strength. Higher aging temperature is observed to be generally reducing the welded specimen fatigue strength (figure 48). Also, it is noticed that for the same aging condition, the welded specimens always gave lower fatigue strength as compared to regular specimens (figure 59-52). The metallurgical changes that normally accompany the process of welding are considered to be causing this fatigue strength reduction. The Heat Affected Zone of the welded specimen was generally the site for the fatigue crack to form. At this HAZ, sensitization is believed to have occurred which lead to extensive carbide precipitation which in turn have lead to further reduction to the fatigue strength when compared to regular un-welded specimens.

5.6 Conclusions:

This study has outlined the effect of the aging treatment on the fatigue strength of alloy 800HT. The following conclusions can be drawn from the study:

1. The fatigue strength has shown a general reduction with increased aging temperature.
2. The aging treatment produced various amounts of carbide precipitate (mainly chromium enriched carbide precipitates) at the grain boundary, twin boundary and intra-granular regions.
3. These carbides, examined under SEM, are noticed to increase in size and quantity with higher aging temperature and are believed to be contributing to the reduction in fatigue strength of the alloy.

4. This reduction in fatigue strength is believed to have come about by the formation of secondary cracking triggered during fatigue testing by the same carbide precipitates.
5. Extensive secondary cracking was associated with extensive carbide precipitation and with reduced fatigue strength.

5.7 Proposed Future Work:

High temperature fatigue testing was not conducted due to the lack of the high temperature fatigue testing facilities and is recommended as future work in this area. The result of such high temperature fatigue study can then be compared to the data outlined in this study in order to understand the effect of high temperature fatigue and creep-fatigue interaction.

Table 1: Heat-Treatment Regimes.

Aging Condition	Temperature °C	Hours (Hr)
A1	650	24
A2	760	24
A3	870	24
A4	650	100
A5	760	100
A6	870	100
A7	650	500
A8	760	500
A9	870	500
A10	650	1000
A12	870	1000

Table 2: Chemical composition of alloy 800HT.

Element	% Composition
C	0.074
Si	0.52
Mn	0.72
S	0.001
AL	0.54
Co	0.58
Cr	20.0
Cu	0.36
Fe	45.22
Ni	31.14
Ti	0.46
Ni +Co	31.72
Ti+Al	1.00

Table 3: Mechanical properties of alloy 800HT @ 20° C

.2% proof strength	211 MPa
Tensile strength	554 Mpa
% Elongation - on 50mm	45.5
Hardness	150/162 hv-30

Table 4: Fatigue data of as-received (AR) and solution treated (S2) specimens.

Load KN	Stress MPA	AR Life Cycle	S2 life Cycle
5	166.7		
6	200		
7	233.33		
8	266.7	2000000	2000000
10	333.3	1375451	635398
12	400	412993	220876
13	433.3		
14	466. 7	159257	54211
15	500	133181	
16	533. 3		20592
17	566. 7		

Table 5: Fatigue data of specimens aged for 24 hours at 650°C, 760°C and 870°C (A1, A2, and A3) respectively.

Load KN	Stress MPA	A1 Life Cycle	A2 Life Cycle	A3 Life Cycle
5	166.667			3000000
6	200	3000000	2000000	
7	233.3		663730	2946551
8	266.7		497245	314176
10	333.3	135399	197092	135037
12	400	120992	96978	92826
13	433.3		89022	58873
14	466.7	63117	72828	75640
15	500	35174	22664	50507
16	533.3		13796	
17	566.7	29869		

Table 6: Fatigue data of specimens aged for 100 hours at 650°C, 760°C and 870°C (A4, A5, and A6) respectively.

Load KN	Stress MPA	A4 Life Cycle	A5 Life Cycle	A6 Life Cycle
5	166.7			
6	200			1040453
7	233.3			
8	266.7	3000000		131494
10	333.3	409979	223844	123695
12	400	216954	156922	46999
13	433.3			
14	466.7	161739		75962
15	500	135853	88473	77480
16	533.3	119236	63347	51834
17	566.7	91076	26852	38146

Table 7: Fatigue data of specimens aged for 500 hours at 650°C, 760°C and 870°C (A7, A8, and A9) respectively.

Load KN	Stress MPA	A7 Life Cycle	A8 Life Cycle	A9 Life Cycle
5	166.7			
6	200		3000000	1552385
7	233.3	3000000	844082	
8	266.7	1277986	251115	329623
10	333.3	407549	254292	180967
12	400	144689	114988	
13	433.3	98177	104004	
14	466.7	88387	55322	38007
15	500	80585	53486	7989
16	533.3	52885	15885	
17	566.7			

Table 8: Fatigue data of specimens aged for 1000 hours at 650°C and 870°C (A10 and A12) respectively.

Load KN	Stress MPA	A10 Life Cycle	A12 Life Cycle
5	166.7		
6	200		3000000
7	233.3		
8	266.7	2000000	344304
10	333.3	2000000	351336
12	400	351987	80295
13	433.3	266077	61405
14	466.7	275568	96739
15	500	175376	27154
16	533.3	126364	
17	566.7		

Table 9: Fatigue data of welded As-Received and Welded specimens aged for 100 hours at 650°C, 760°C and 870°C (ARW, A4W, A5W and A6W).

Load KN	Stress MPA	ARW Life Cycle	A4W Life Cycle	A5W Life Cycle	A6W Life Cycle
5	166.7				
6	200	3000000	3000000		272038
7	233.3				
8	266.667	389942	2450803	62362	65618
10	333.3				
12	400	113010	44741	36507	25704
13	433.3				
14	466.7	24745	18045	23425	21569
15	500				
16	533.3	66440	14340	9545	8225
17	566.7				

Figure 1 Incoloy 800HT Hour-Glass Rupture Fatigue Test Specimen

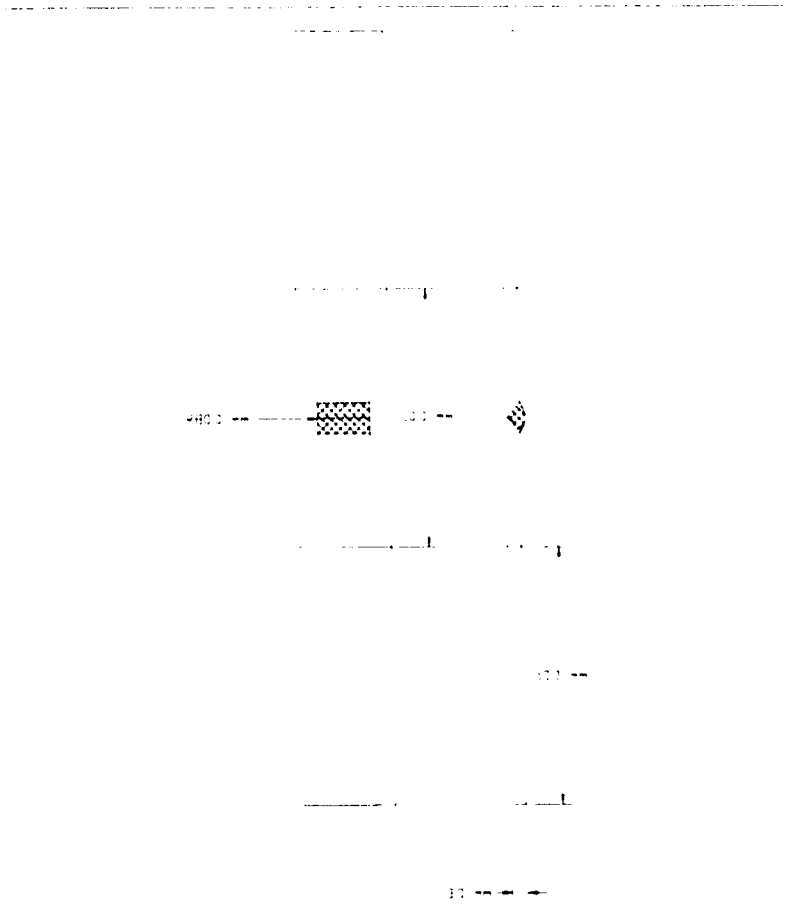

Figure 3 Inconel 600H™ round-bar welded fatigue test specimen

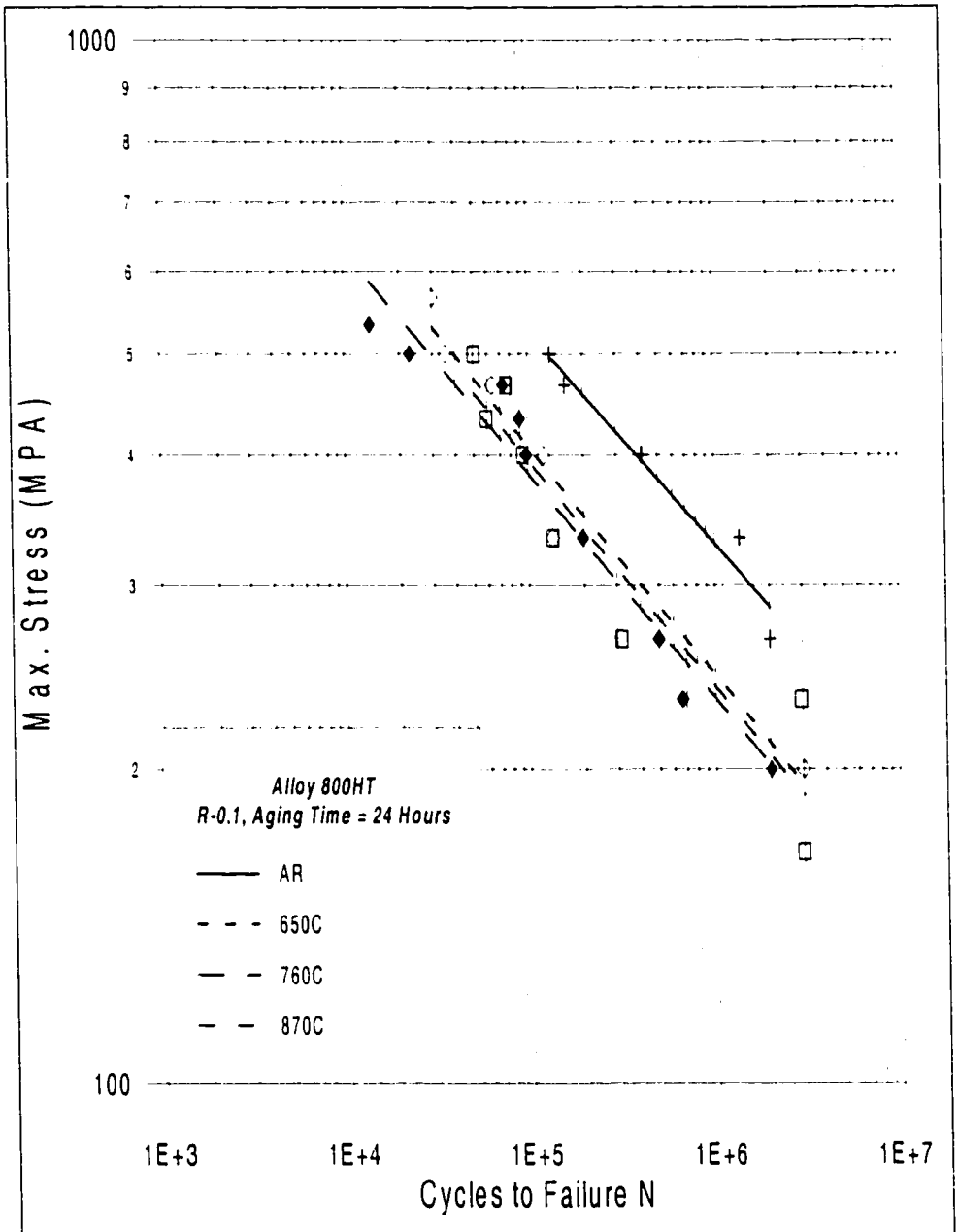

Figure 3: The effect of temperature on the fatigue strength at 24 hours aging time.

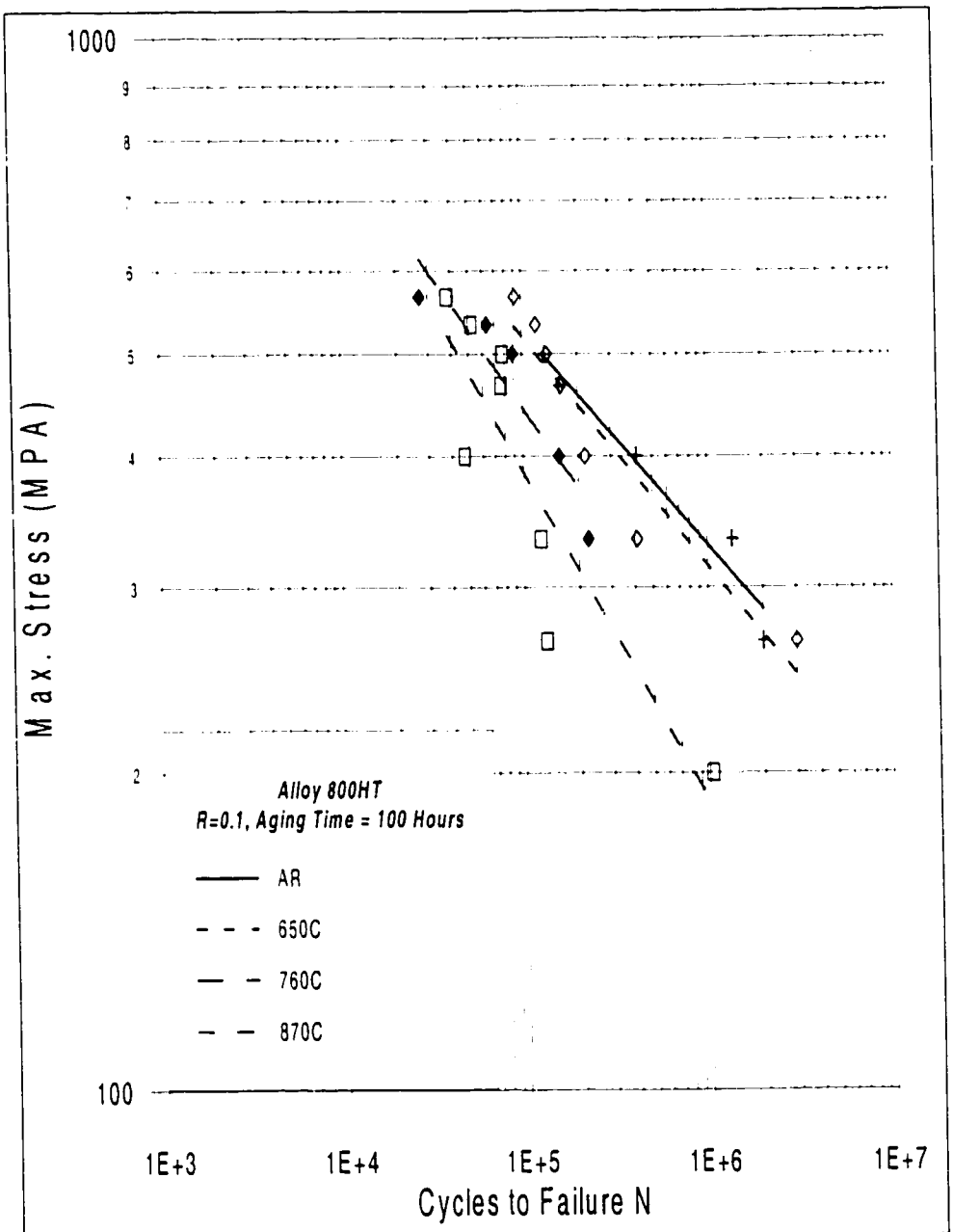

Figure 4: The effect of temperature on the fatigue strength at 100 hours aging time

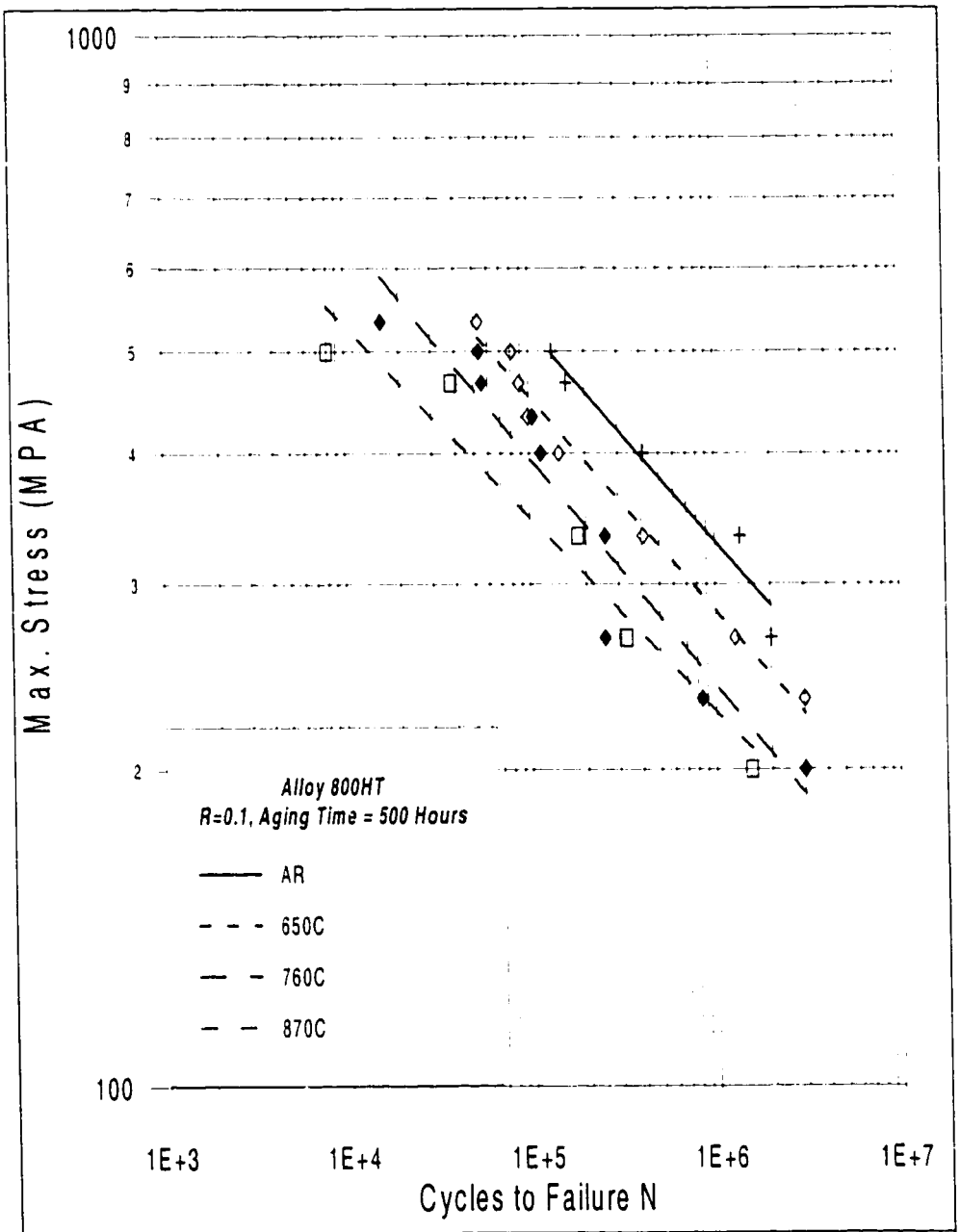

Figure 5: The effect of temperature on the fatigue strength at 500 hours aging time

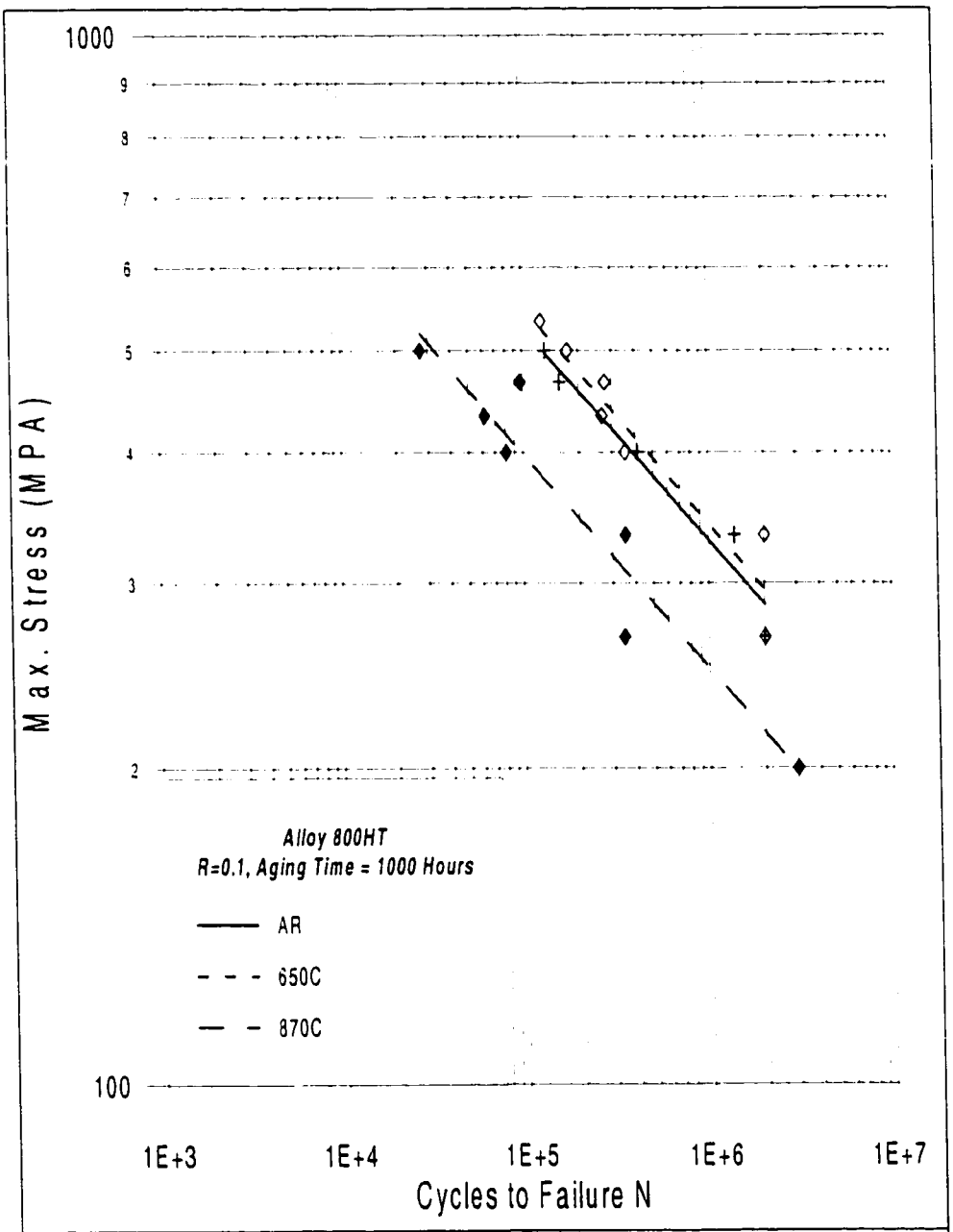

Figure 6: The effect of temperature on the fatigue strength at 1000 hours aging time

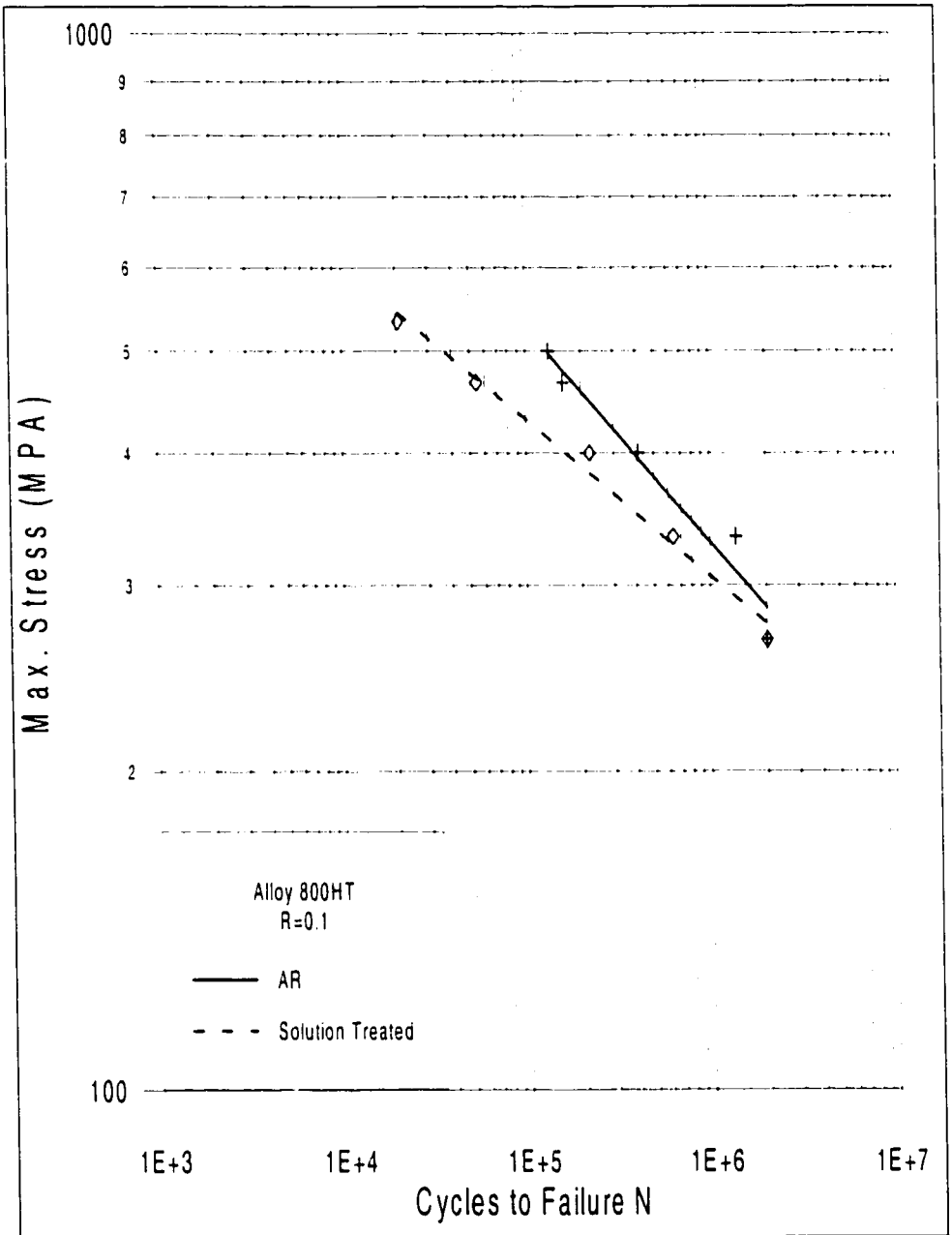

Figure 7: Fatigue data of As-Received compared to Solution Treated material.

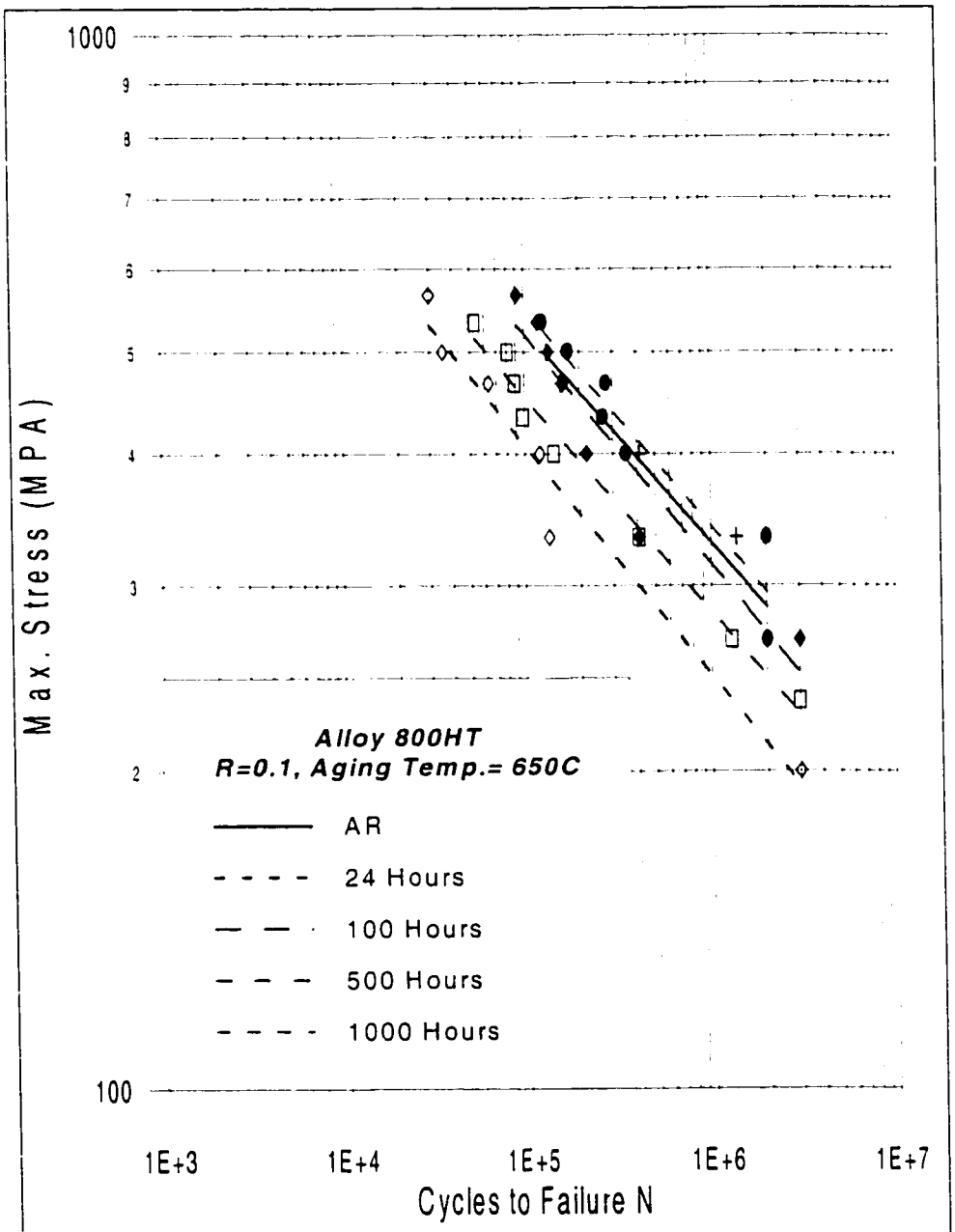

Figure 8: The effect of time on the fatigue strength at 650°C aging temperature

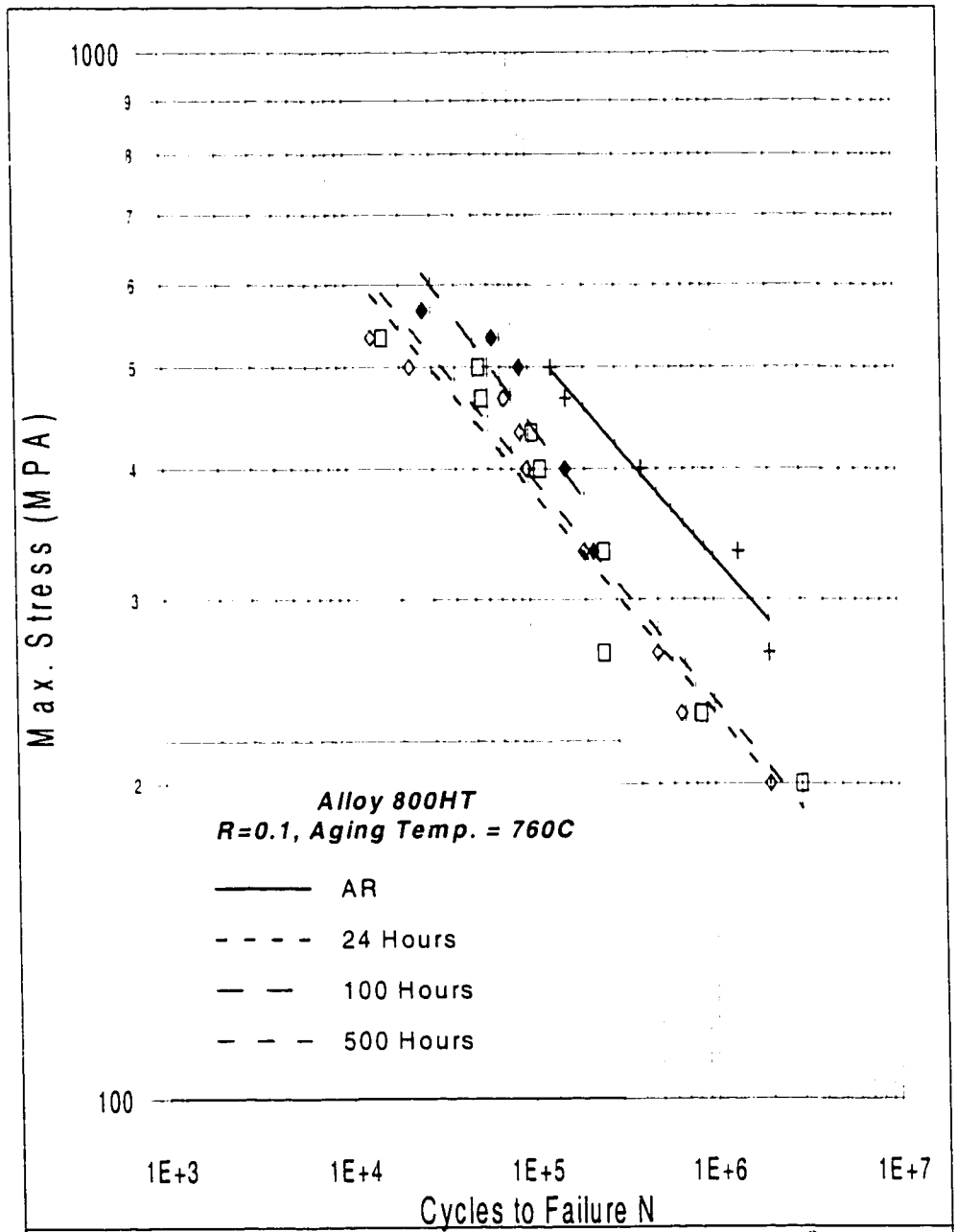

Figure 9: The effect of time on the fatigue strength at 760°C aging temperature.

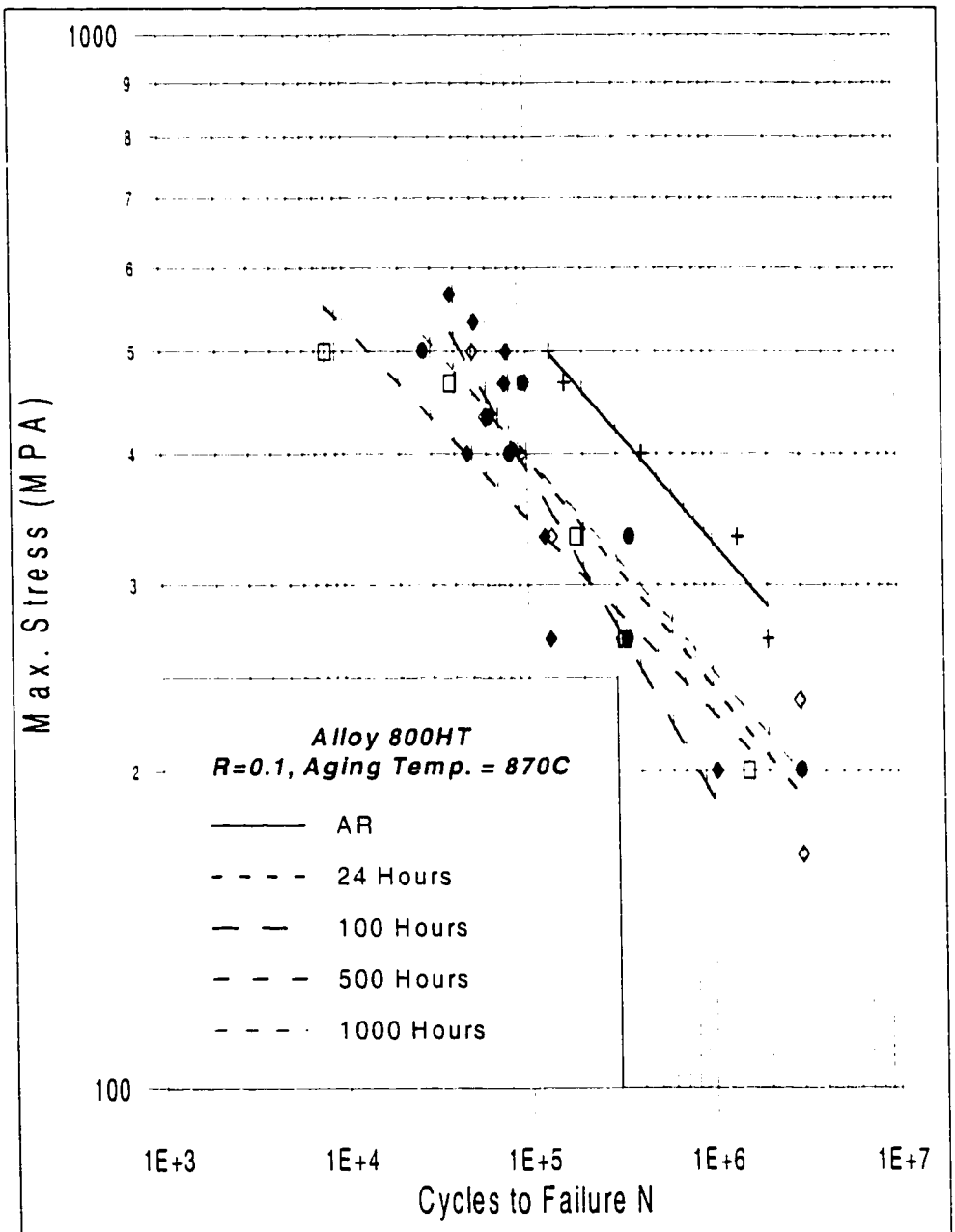

Figure 10: The effect of time on the fatigue strength at 870°C aging temperature.

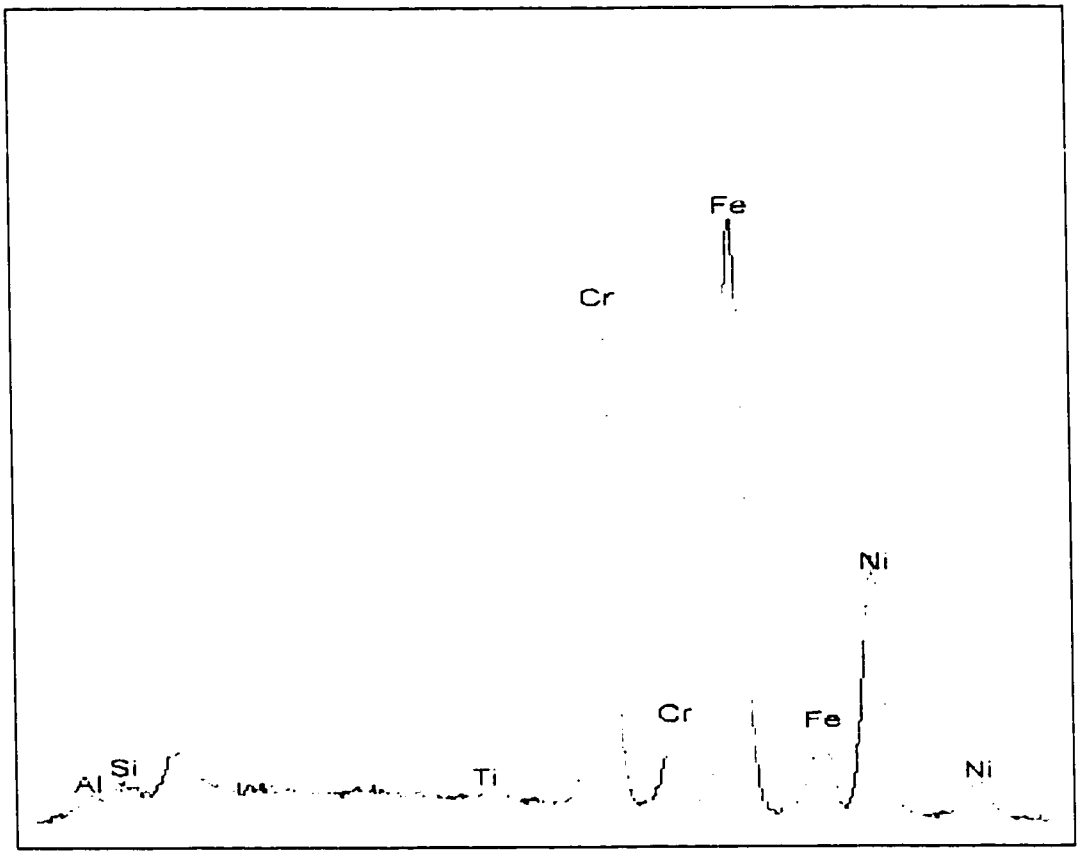

Figure11: EDS Spectrograph showing base material element concentrations. The weight element concentration of the quantified test showed equivalent % to the vendor supplied data.

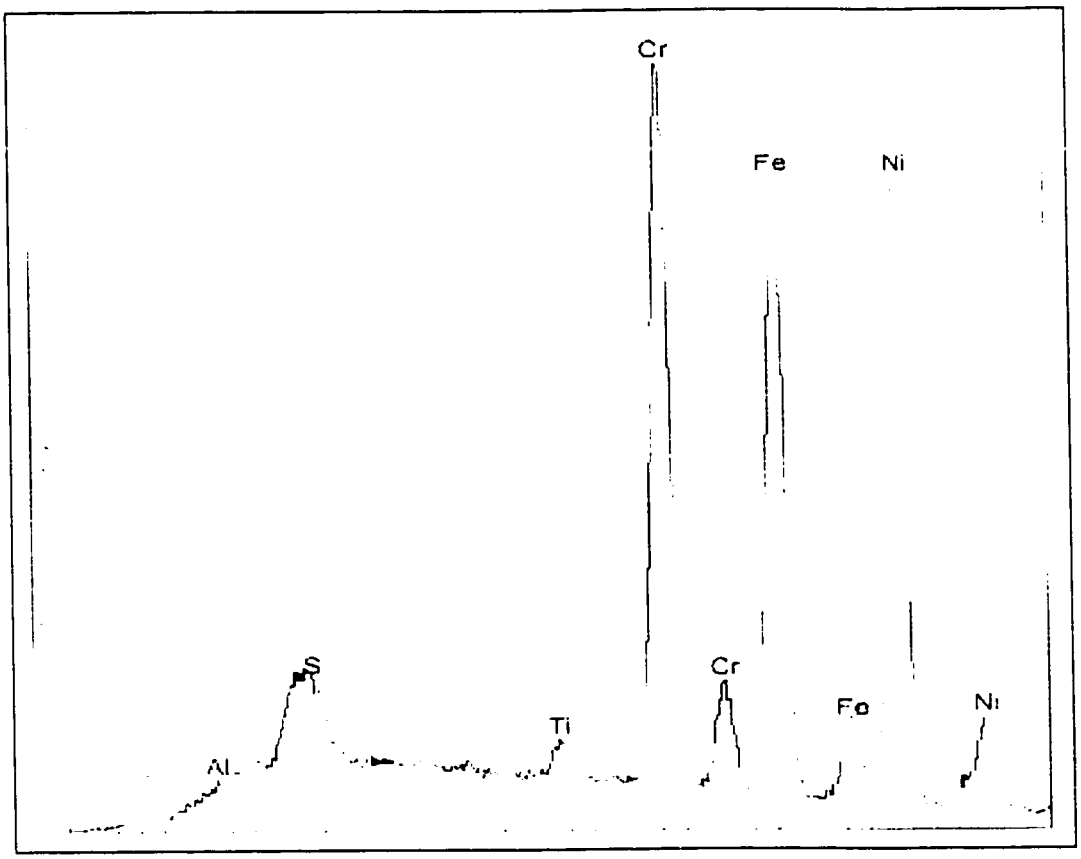

Figure 12: EDS Spectrograph showing grain boundary element concentrations with high Chromium concentration. The increase in %Cr is attributed to the formation of $M_{23}C_6$ Type carbide precipitates.

Figure 13: Micrograph of specimen aged at 650 °C for 24 hours (5000X). The grain boundary regions contain only small amounts of discontinuous carbide precipitates (A), whereas the grains are clear of any carbide precipitate formation (B).

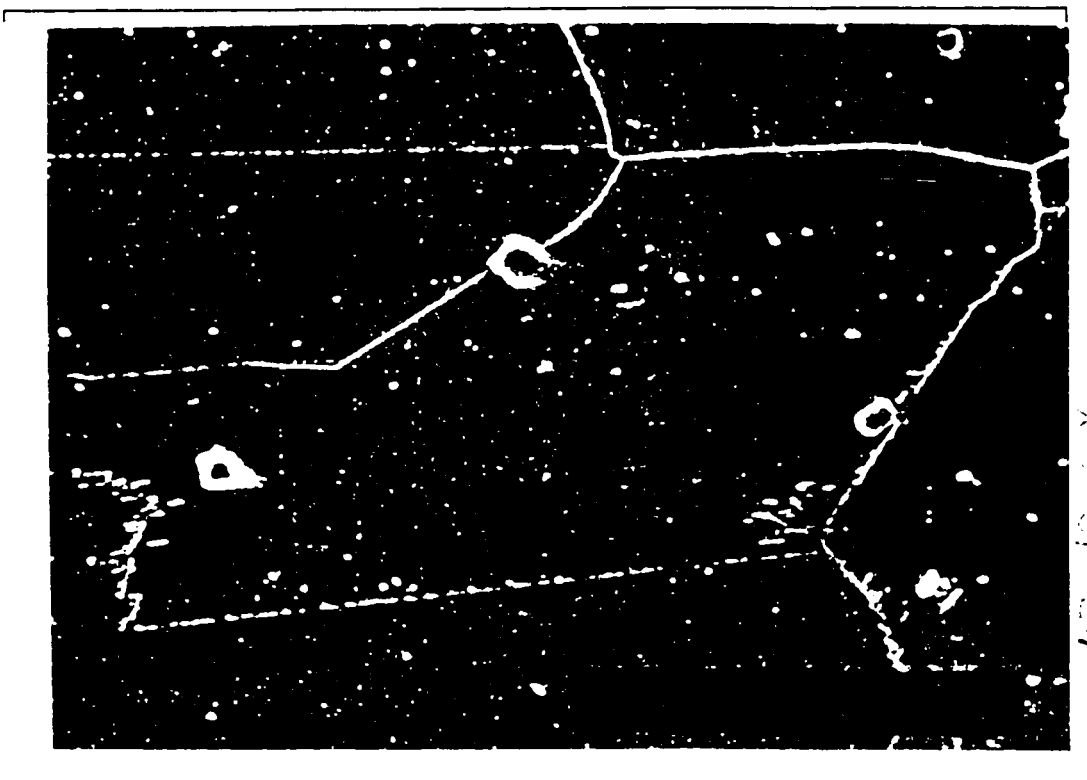

Figure 14: Micrograph of specimen aged at 870°C for 24 hours (1000X). This microstructure clearly shows the effect of aging on the precipitate formation. Aging at 870°C has caused the formation of fine semi-continuous network of grain boundary precipitates (A), intra-granular carbide precipitates (B), and discontinuous twin boundary network(C). The TiC carbides are also visible randomly scattered in the alloy matrix (D).

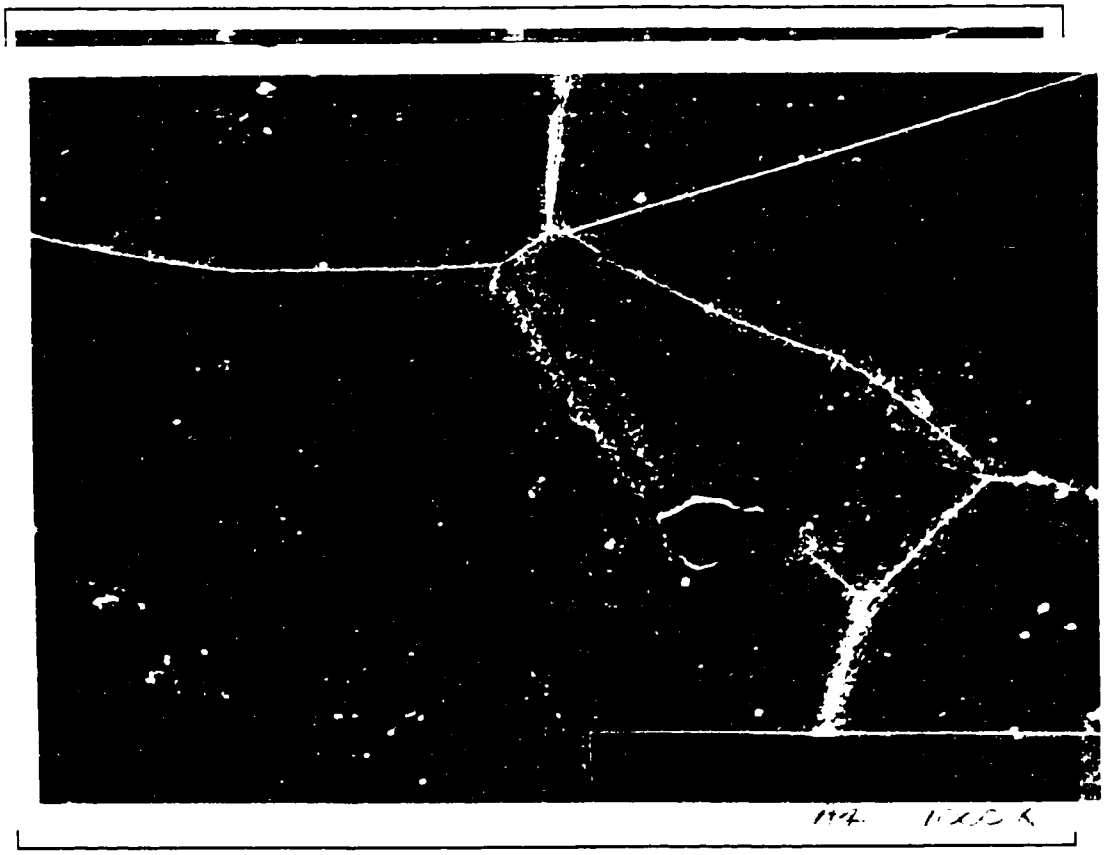

Figure 15: Micrograph of specimen aged at 650°C for 100 hours (1000X). A fine continuous network of carbide precipitates is observed at the grain boundary regions (A). The TiC carbides (B) are noticed to be stable through the various aging treatments. Small amounts of intra-granular carbides start to form at after 100 Hours of aging at 650°C (C). There is no observed carbide formation at this aging treatment.

Figure 16: Micrograph of specimen aged at 760°C for 100 hours (200X). Somewhat thicker network of grain boundary carbides precipitates are observed at this aged specimen (A). Small amounts of carbides are also noticed at the twin boundary regions (B and C) and inside the grains (D).

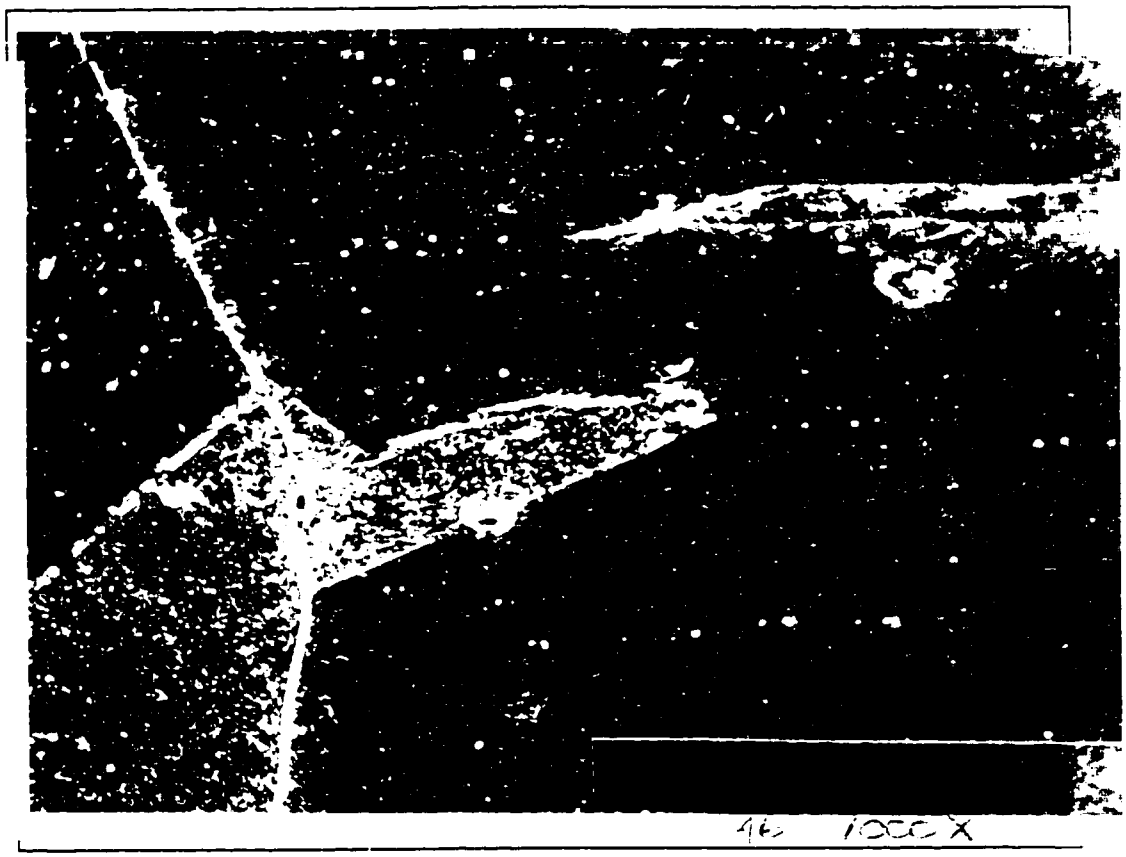

Figure 17: Micrograph of specimen aged at 870°C for 100 hours (1000X). Aging at 870°C has clearly caused thicker carbide precipitation at the grain boundary regions (A) and at the twin boundary regions (B). The intra-granular carbide precipitation has also shown to increase in quantity (C), as compared to the aging at lower temperatures.

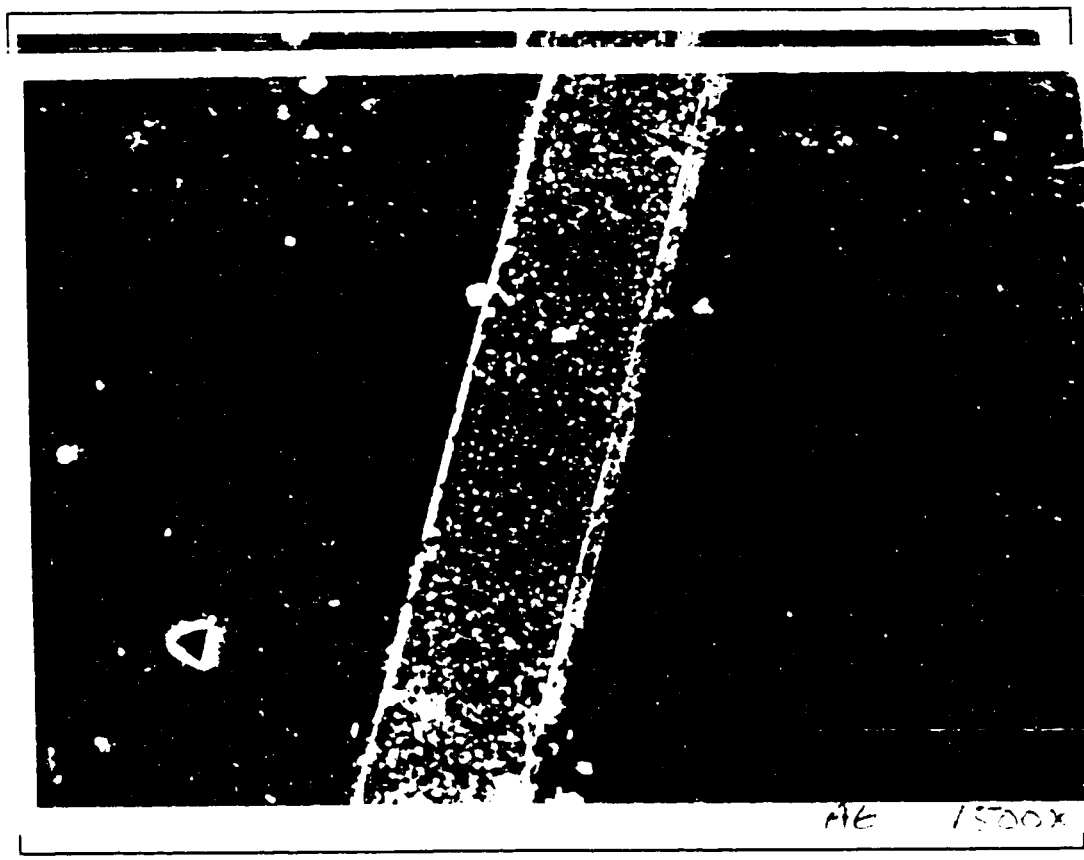

Figure 18: Micrograph of specimen aged at 870°C for 100 hours (1500X). A closer look at the twin boundary carbide precipitates (A). The TiC carbides (B) can also be observed to be stable through these aging treatments.

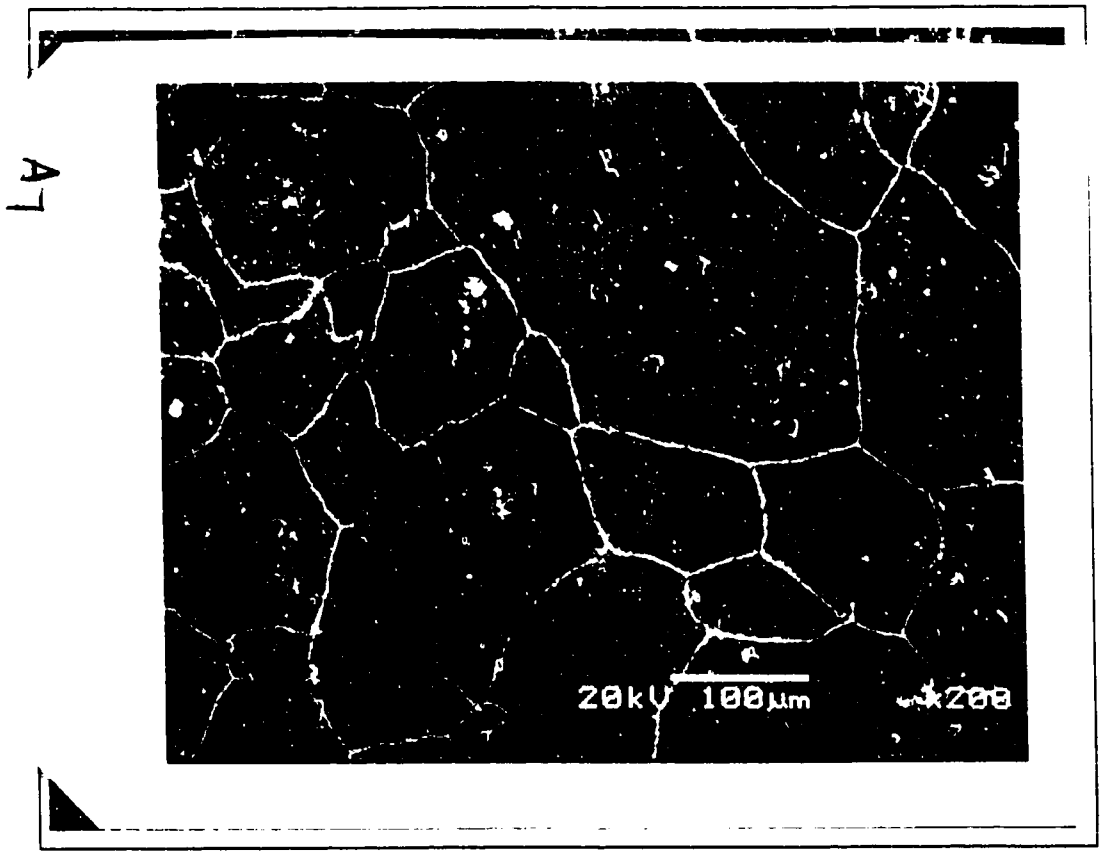

Figure 19: Micrograph of specimen aged at 650°C for 500 hours (200X). Even with longer aging time of 500 hours, the grain boundary regions have only experienced the formation of fine network of carbide precipitation (A). The structure is noticed to be free of twin boundary carbides or any considerable amounts of intra-granular carbides.

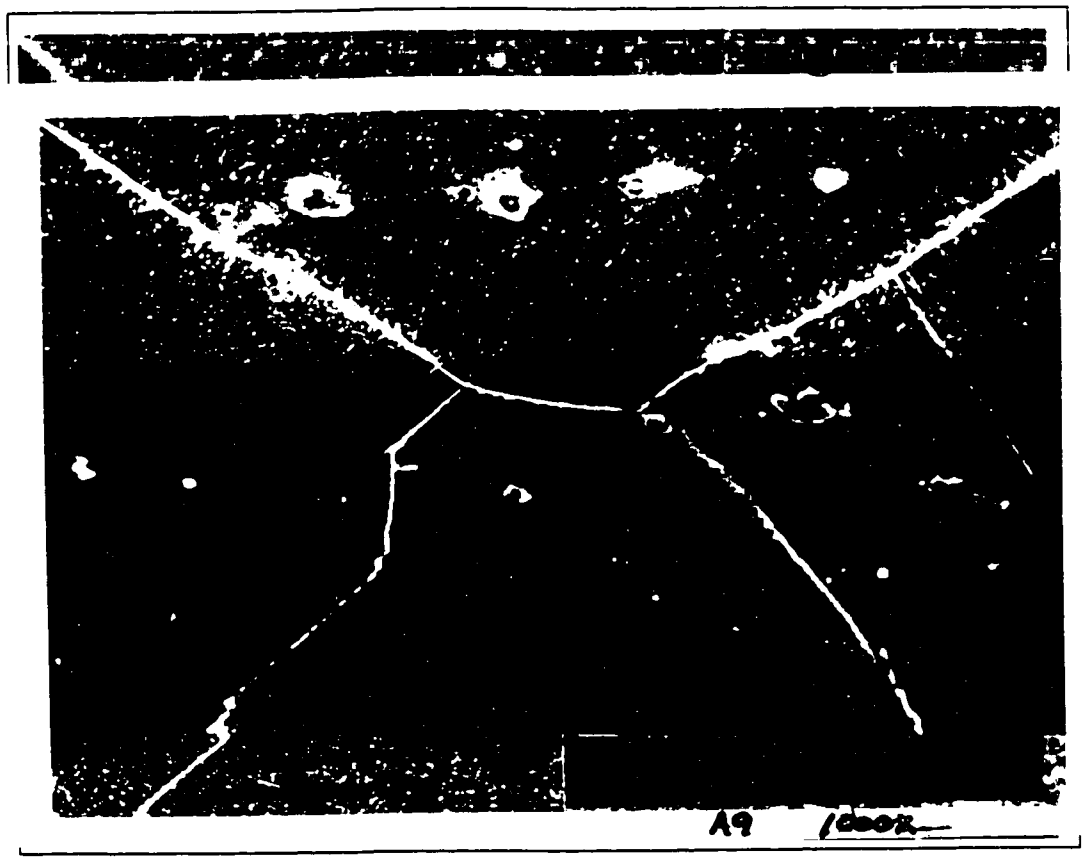

Figure 20: Micrograph of specimen aged at 870°C for 500 hours (1000X). Heavy carbide precipitation is observed at the grain boundary regions (A and B). Location (A) also show the high concentration of carbide precipitates near the grain boundary regions. This is believed to be caused by the high density of dislocation at these areas. Fine continuous of precipitates are observed at the Twin boundaries (C). The TiC carbides are showing the same stability (D).

Figure 21: Micrograph of specimen aged at 650°C for 1000 hours (200X). A fine network of grain boundary carbide precipitates (A) with small amounts of intr-granular carbides (B). Discontinuous twin boundary carbide network (C and D).

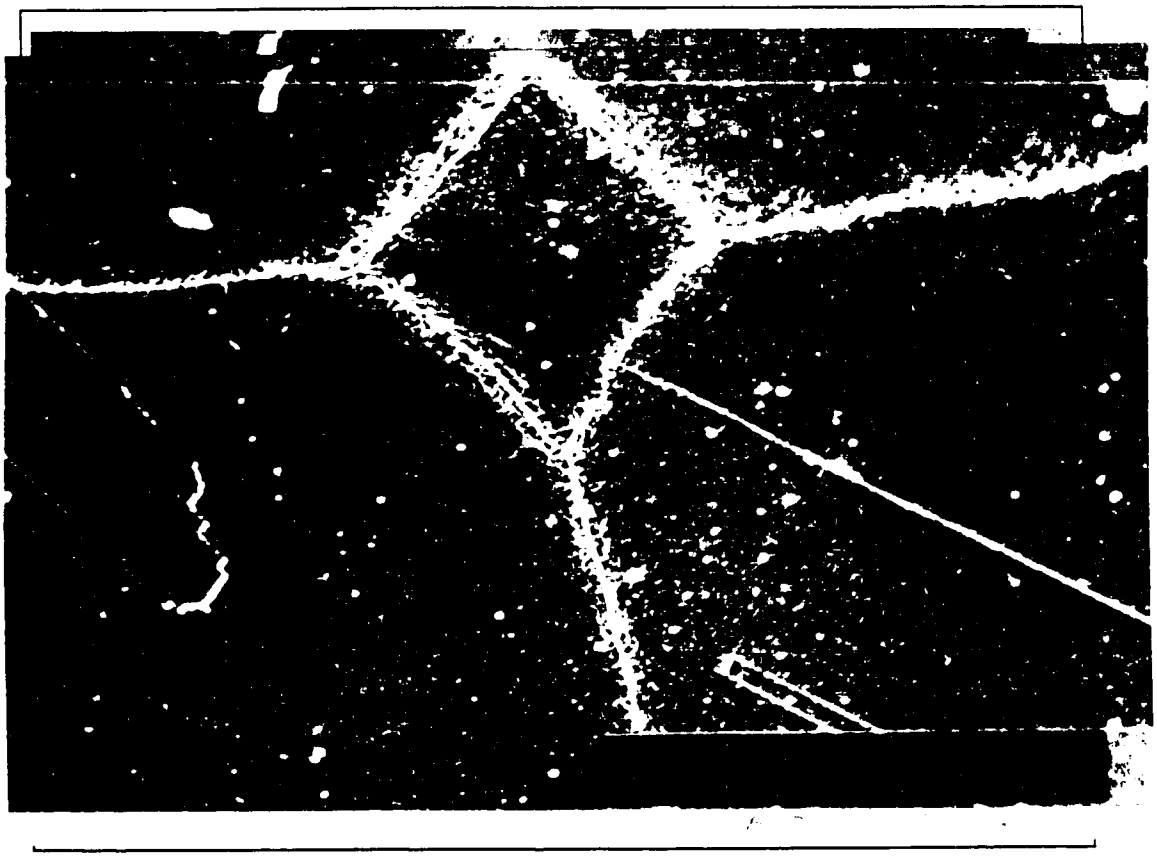

Figure 22: Micrograph of specimen aged at 650°C for 1000 hours (1000X). After 1000 hour of aging at 650°C we observe a fine network of carbide precipitates at the grain boundary regions (A) with small amounts of intra-granular carbides (B). The twin boundary regions contain a fine discontinuous network of carbide precipitates (C and D).

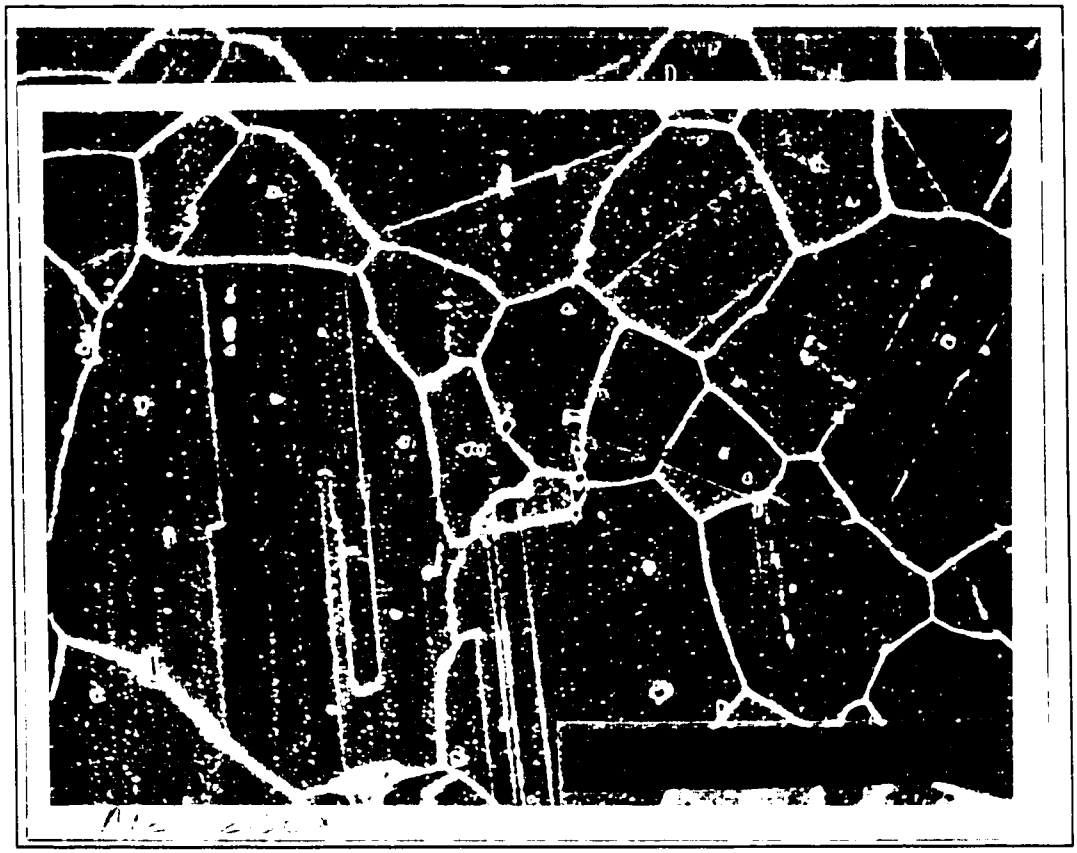

Figure 23: Micrograph of specimen aged at 870°C for 1000 hours (200X). Relatively thicker grain boundary network of precipitates is noticed after aging for 1000 hours at 870°C (A and B) with semi-continuous network of twin boundary precipitates (C and D).

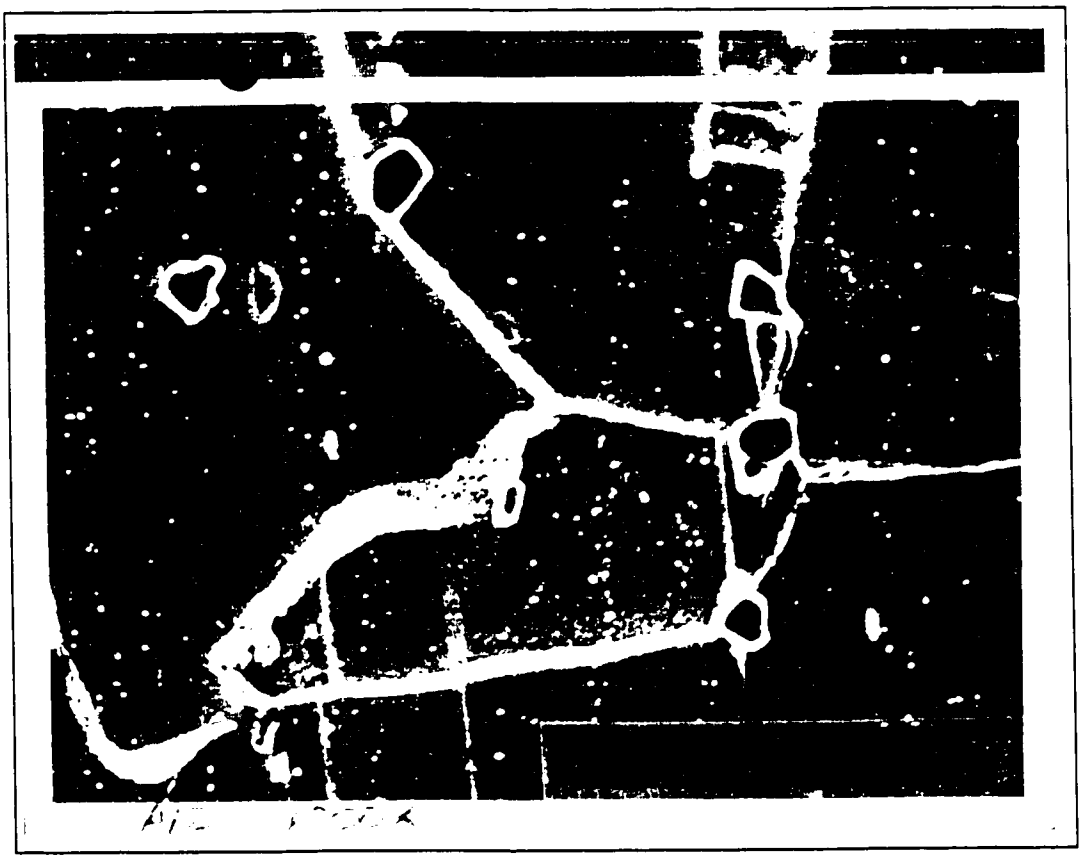

Figure 24: Micrograph of specimen aged at 870°C for 1000 hours (1000X). This is a closer look at the grain boundary precipitates (A) and the intra-granular carbides (B). At this aging condition, new fine TiC carbides start forming mostly at the grain boundary regions (C).

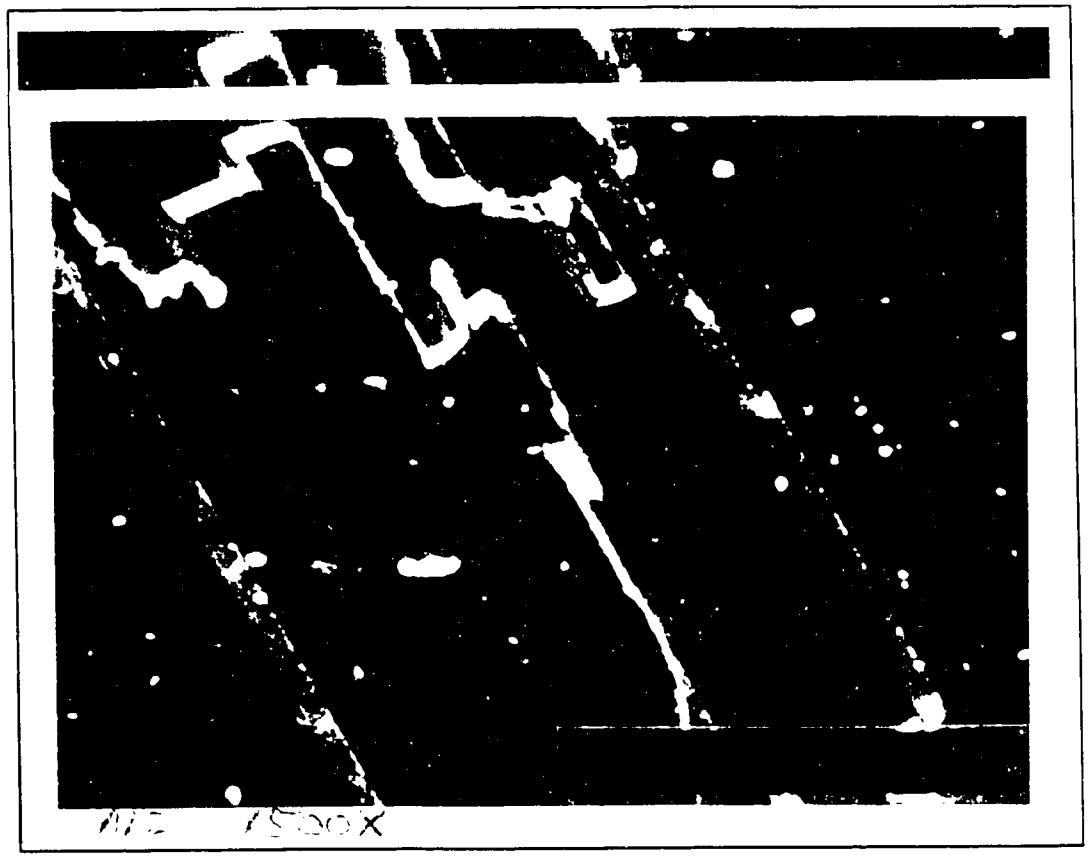

Figure 25: Micrograph of specimen aged at 870°C for 1000 hours (1500X). At this aging condition, heavy twin boundary precipitation (A) as well as an increased intra-granular carbide formation (B) is noticed.

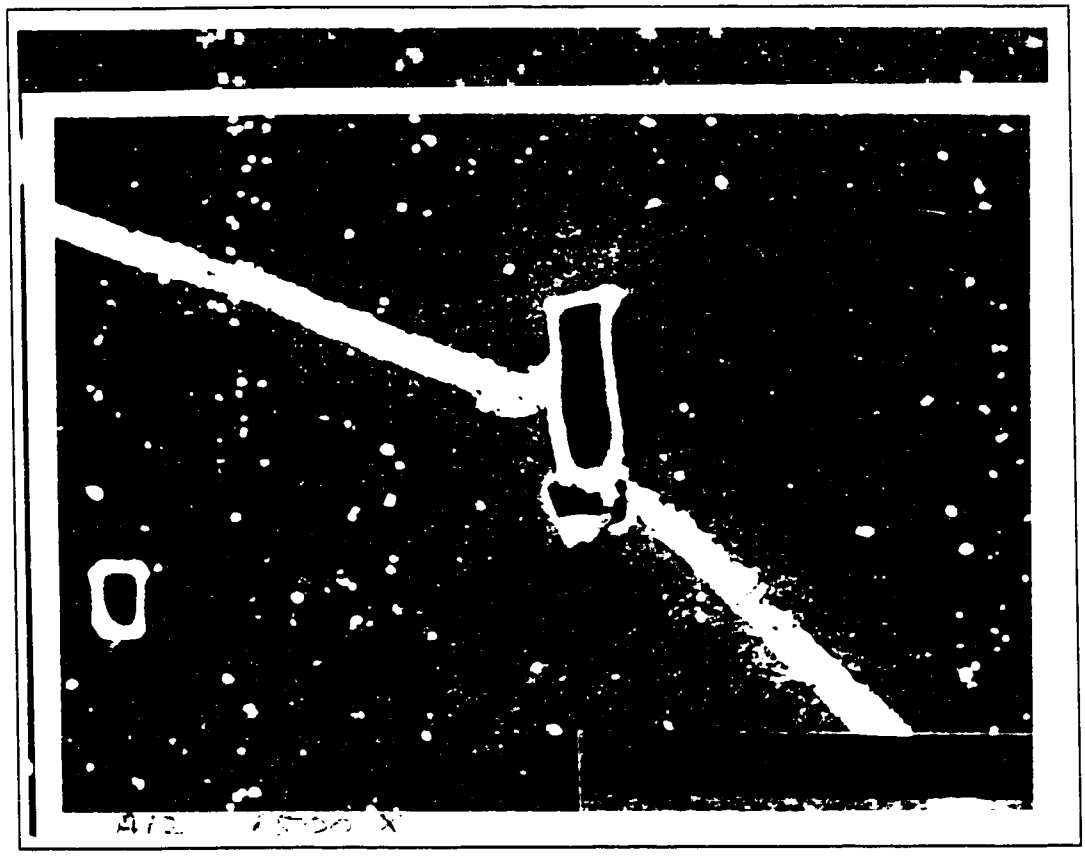

Figure 26: Micrograph of specimen aged at 870°C for 1000 hours (1500X). This micrograph shows the extensive grain boundary carbide precipitation (A) as well as the extensive amounts of intra-granular carbide formation (B). The TiC carbides are shown to be blocky(C).

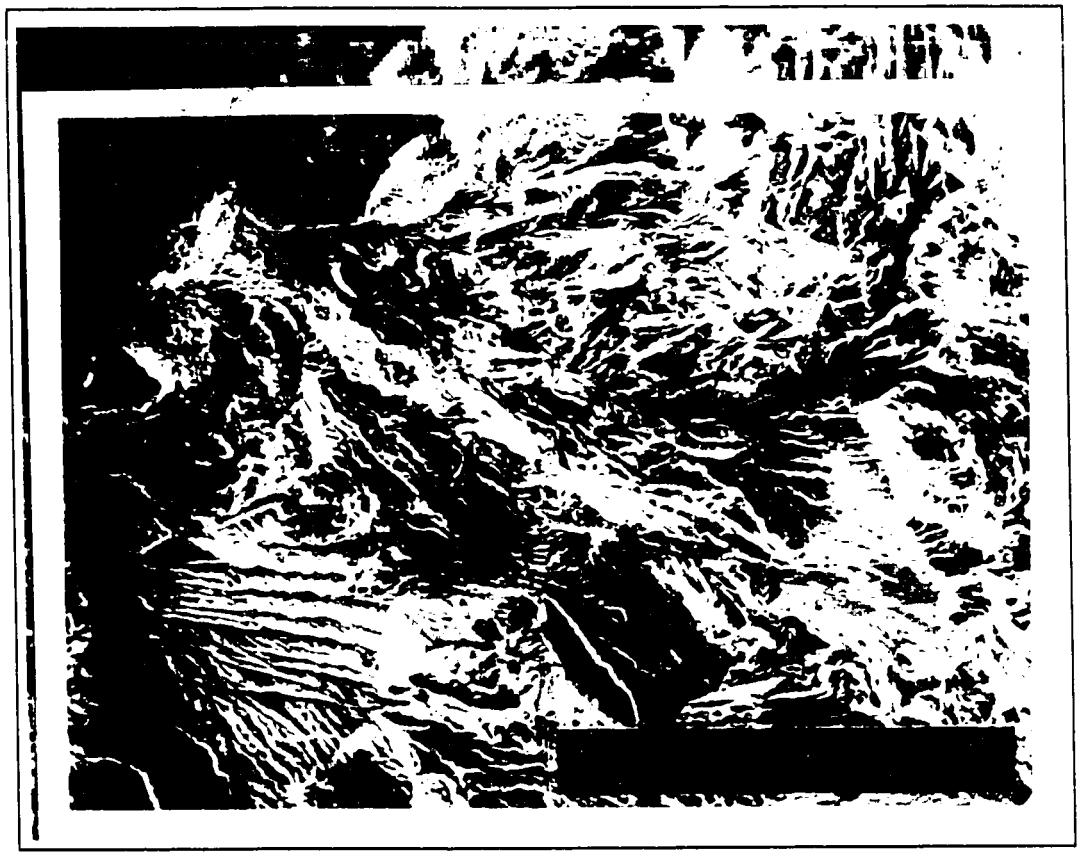

Figure 27: Fracture surface morphology of specimen aged at 650°C for 24 hours. 200X. A very brittle fracture surface showing the initiation region (A), and the propagation region (B). River patterns are noticed in the crack initiation region (C). No considerable secondary cracking is observed at this aged sepecimen.

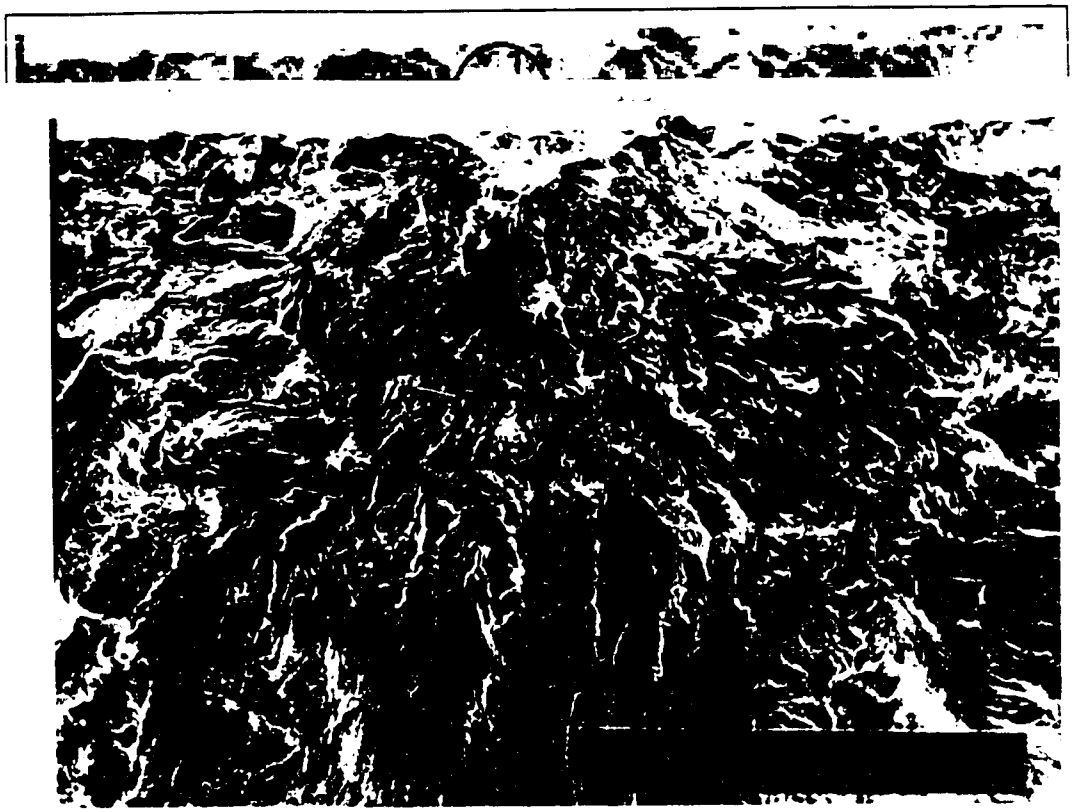

Figure 28: Fracture surface morphology of As-Annealed specimen (50X). A flat brittle crack surface showing the initiaition (A) and propagation (B and C) regions. River patterns are noted in the crack initiation region (A). No considerable cracking observed at this fracture surface.

Figure 29: Fracture surface morphology of specimen aged at 870°C for 500 hours (150X). A rough crack initiation (A) and crack propagation (B) regions. This rough crack propagation region is observed to contain considerably large secondary cracks (B)

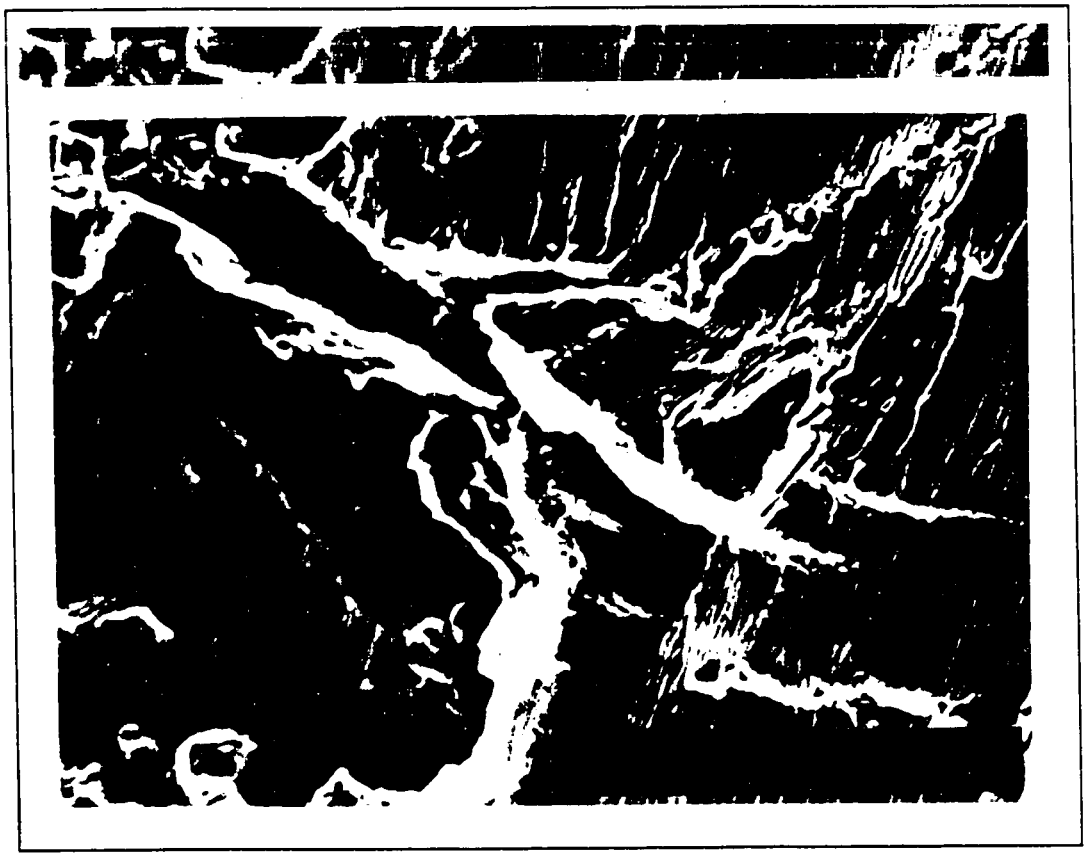

Figure 30: Fracture surface morphology of specimen aged at 650°C for 1000 hours (1000X). Typical fatigue striations (A and B) at the crack propagation regions.

Figure 31 Fracture surface morphology of specimen aged at 870°C for 100 hours (2000X). Typical fatigue striations (A) at the crack propagation region.

Figure 32: Fracture surface morphology of specimen aged at 870°C for 1000 hours (2000X). Typical fatigue striations (A) at the crack propagation region.

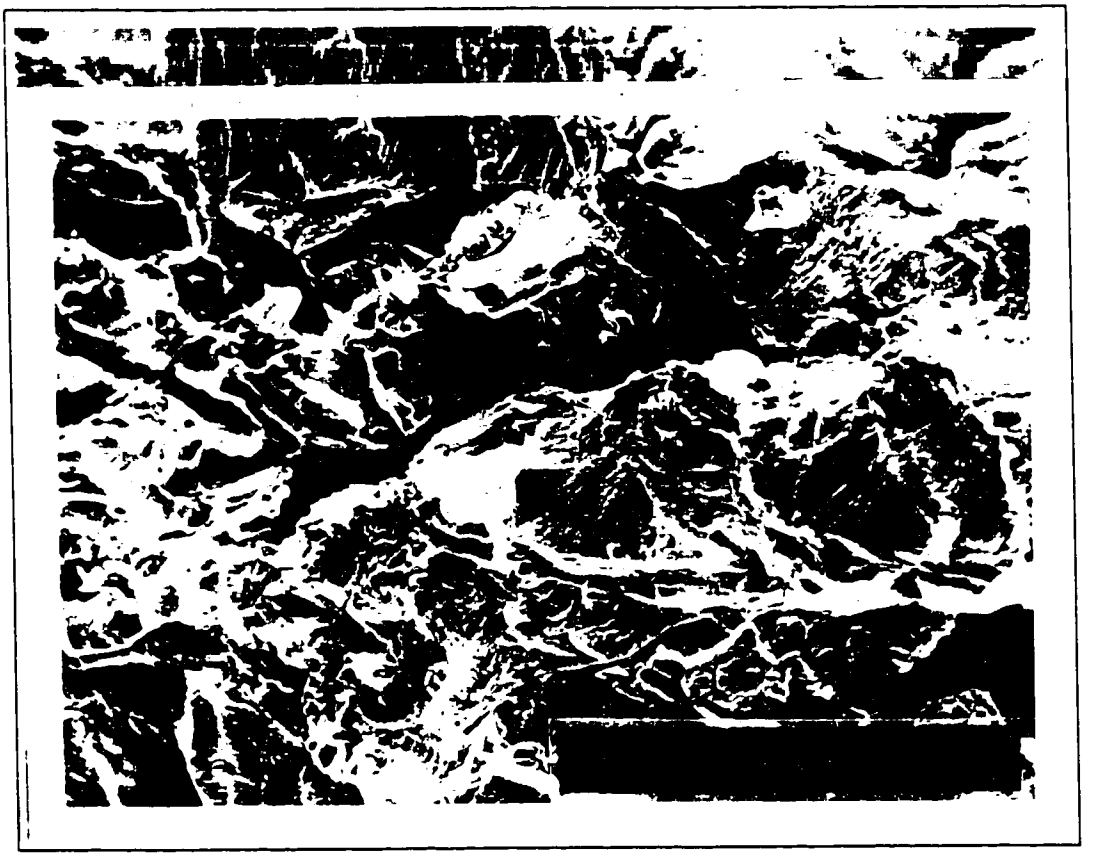

Figure 33: Fracture surface morphology of specimen aged at 870°C for 24 hours (200X). Extensive secondary cracks (A) are observed at the propagation region of this fracture surface (B).

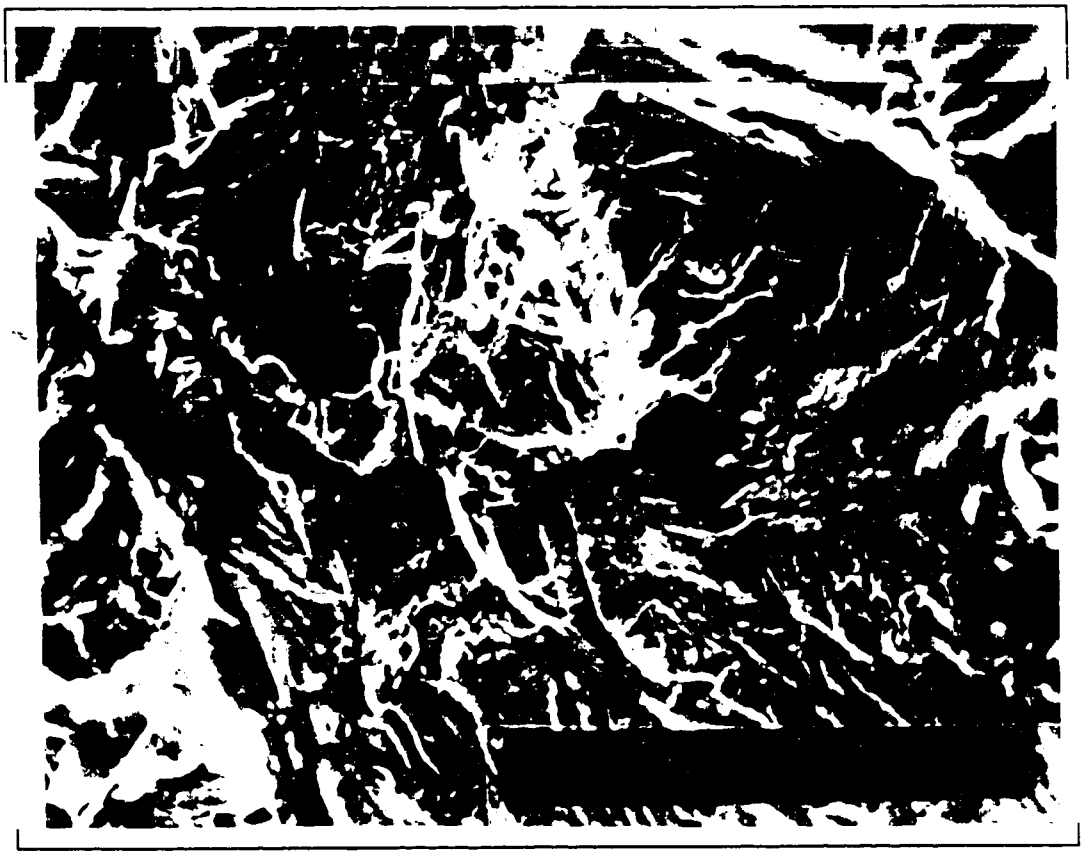

Figure 34: Fracture surface morphology of specimen aged at 760°C for 100 hours (1000X). Large secondary cracks (A) at the crack propagation region.

Figure 35: Fracture surface morphology of specimen aged at 870°C for 500 hours (200X). Rough crack surface with extensive secondary cracks (A, B and C) at the crack propagation region.

Figure 36: Fracture surface morphology of specimen aged at 870°C for 1000 hours (2000X). Extensive secondary cracks (A) at the crack propagation region showing fatigue striations (B).

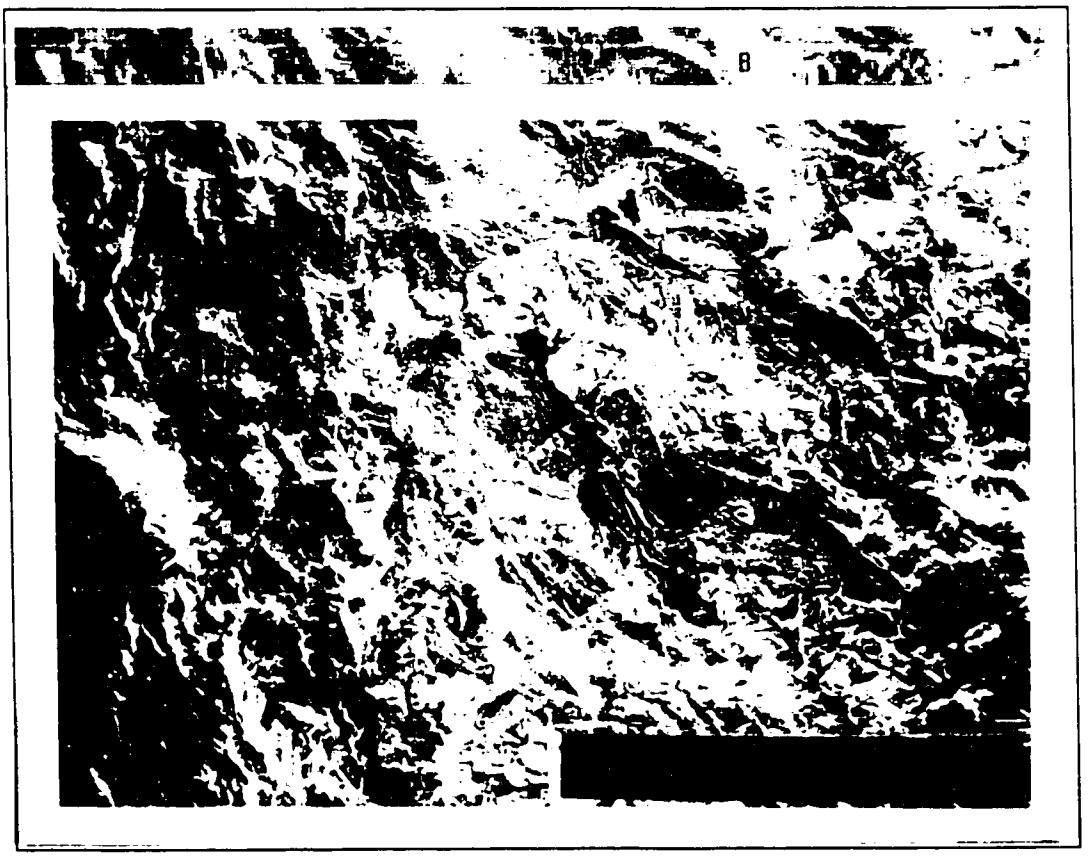

Figure 37: Fracture surface morphology of specimen aged at 870°C for 24 hours (50X). Secondary cracks at this rough crack propagation region (B and C).

Figure 38: Fracture surface morphology of specimen aged at 870°C for 100 hours (200X). Rough crack propagation region (A and C) with secondary cracks (B).

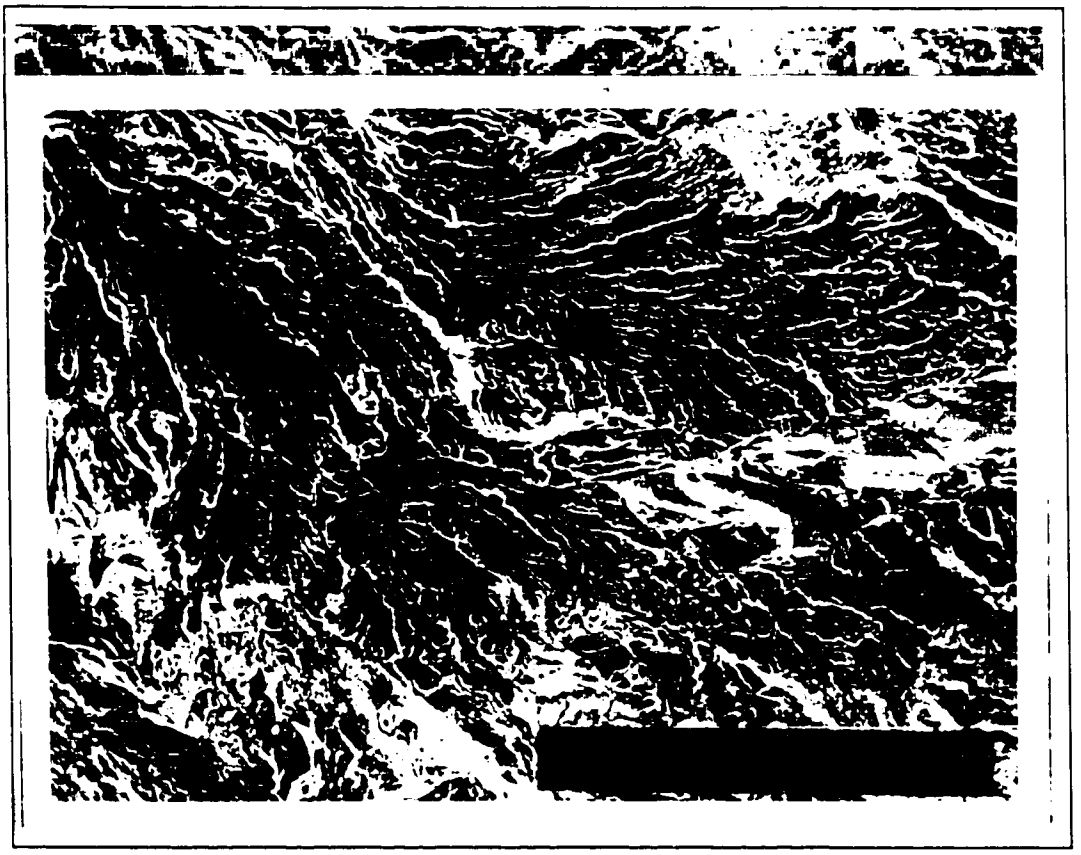

Figure 39: Fracture surface morphology of specimen aged at 650°C for 24 hours (200X). The crack propagation region of a flat brittle fracture surface (A) with no sign of secondary cracking.

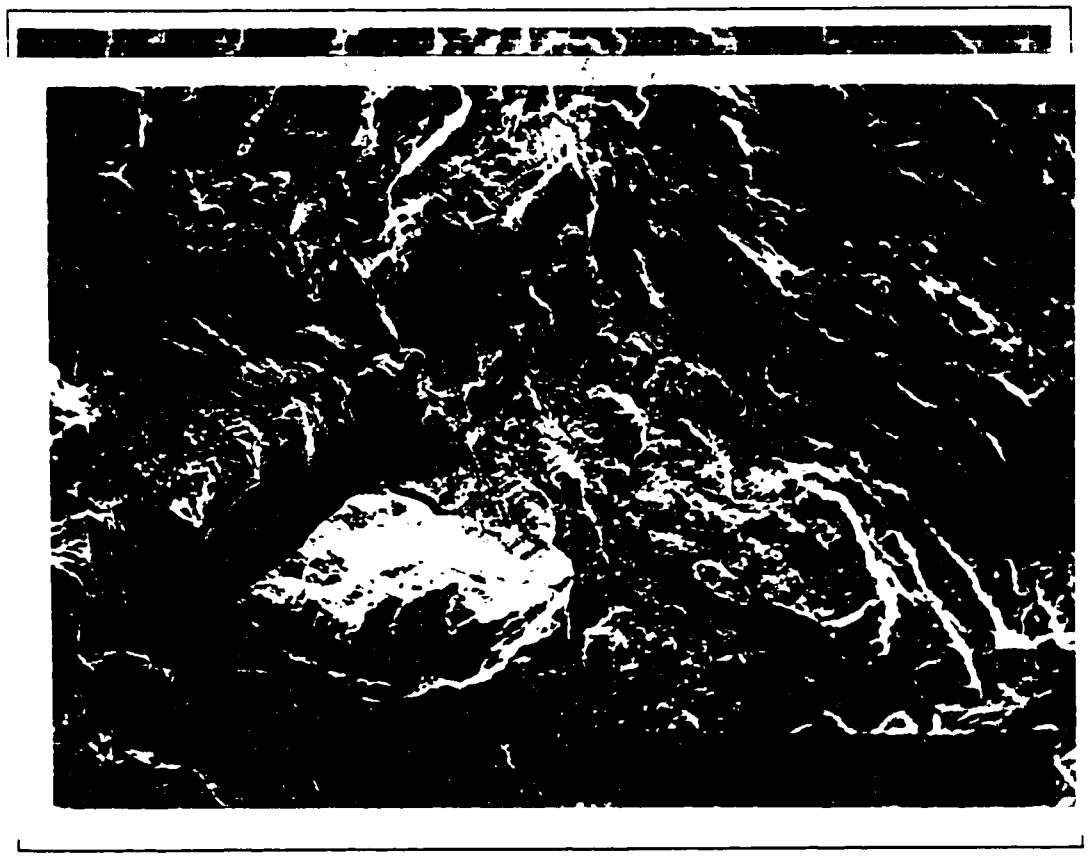

Figure 40: Fracture surface morphology of specimen aged at 760°C for 24 hours (150X). A rough fracture surface with various sizes of secondary cracks (Aand B) in the crack propagation region.

Figure 41: Fracture surface morphology of specimen aged at 650°C for 100 hour (1500X). Small fine secondary cracks (A, B, and C) at a rough crack propagation region.

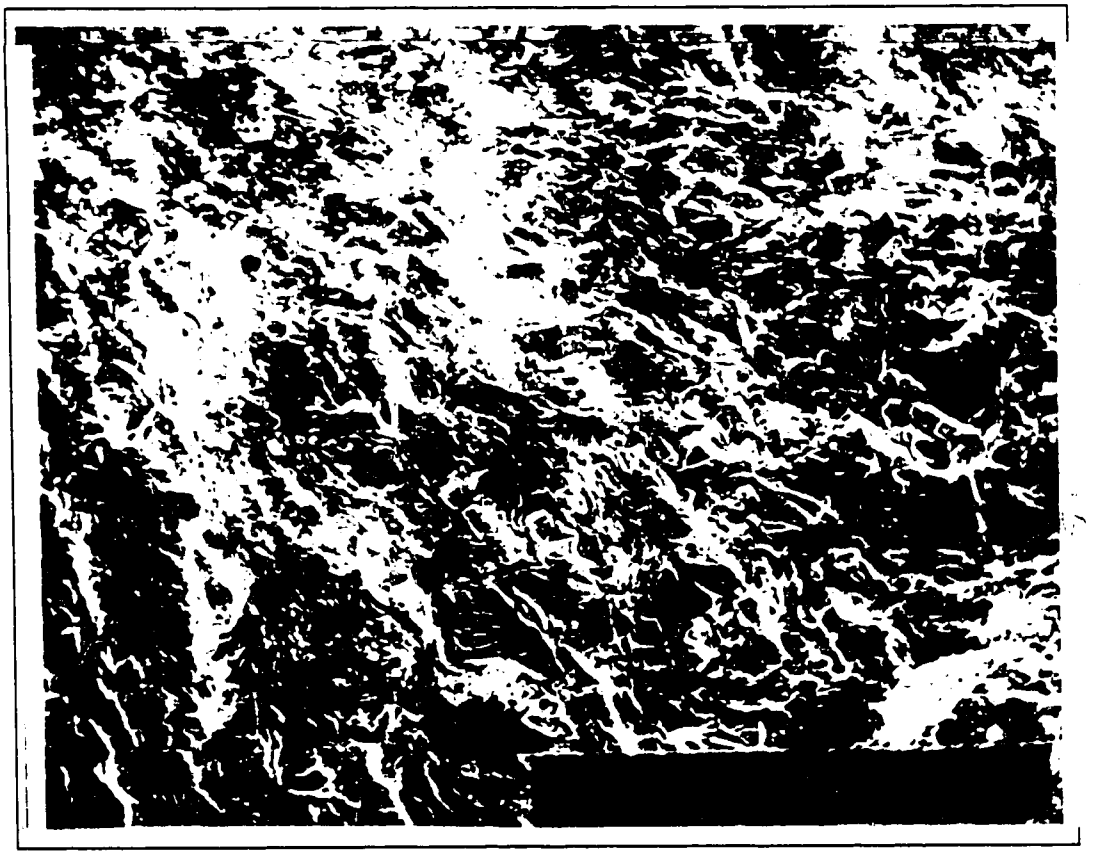

Figure 42: Fracture surface morphology specimen aged at 760°C for 100 hours (35X). Rough crack surface at crack propagation region (A).

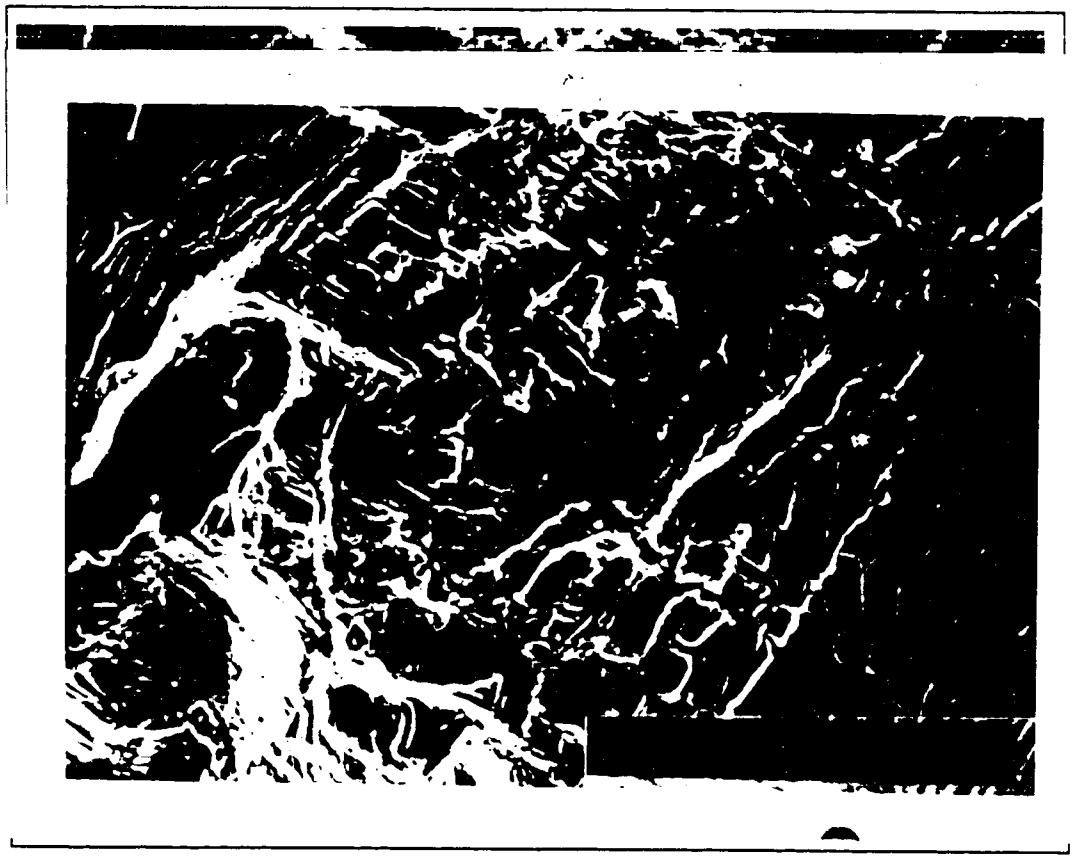

Figure 43: Fracture surface morphology specimen aged at 870°C for 500 hours (1000X). Large amounts of secondary cracks (A, B, and C) at the crack propagation region.

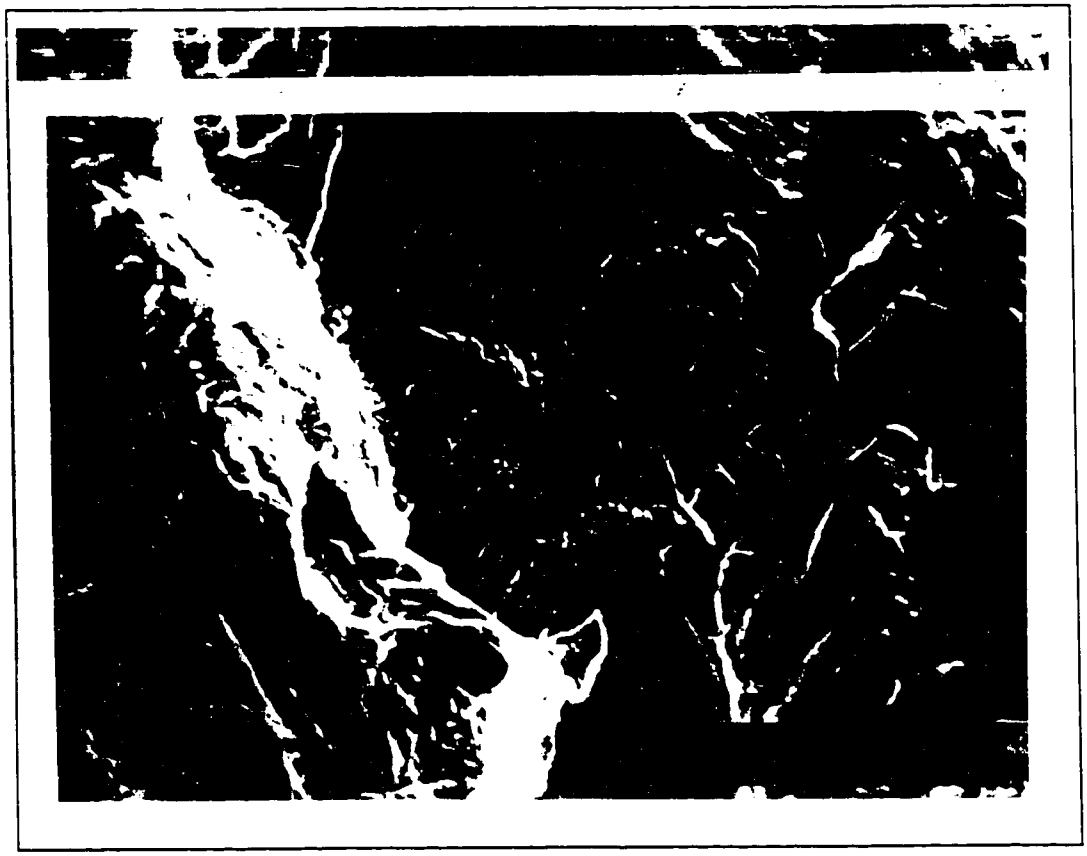

Figure 44: Fracture surface morphology specimen aged at 650°C for 1000 hours (750X). Flat trans-granular crack at the crack propagation region showing typical striations (A) with secondary cracks (B).

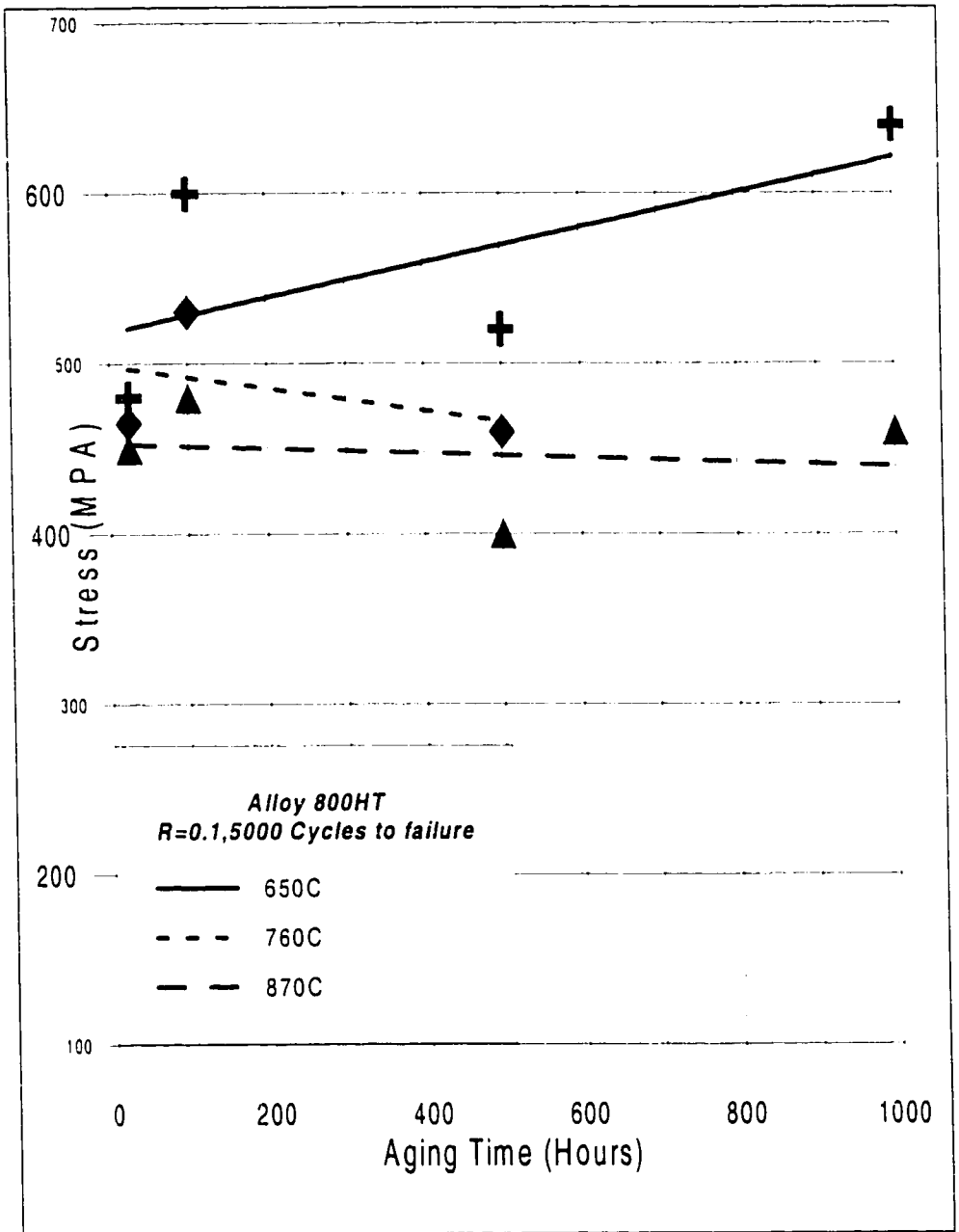

Figure 45: The effect of temperature on fatigue strength at N = 5,000

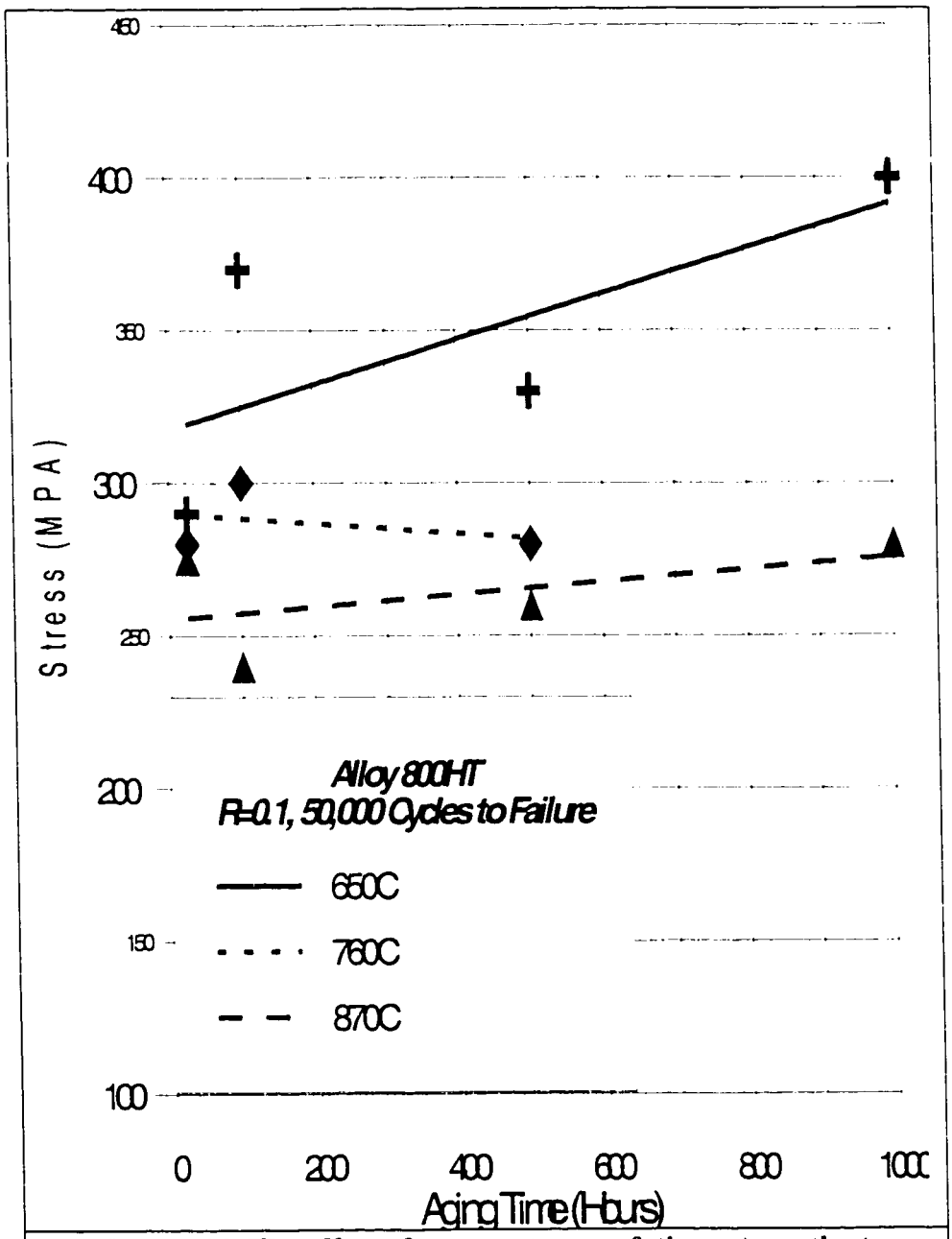

Figure 46: The effect of temperature on fatigue strength at N = 50,000

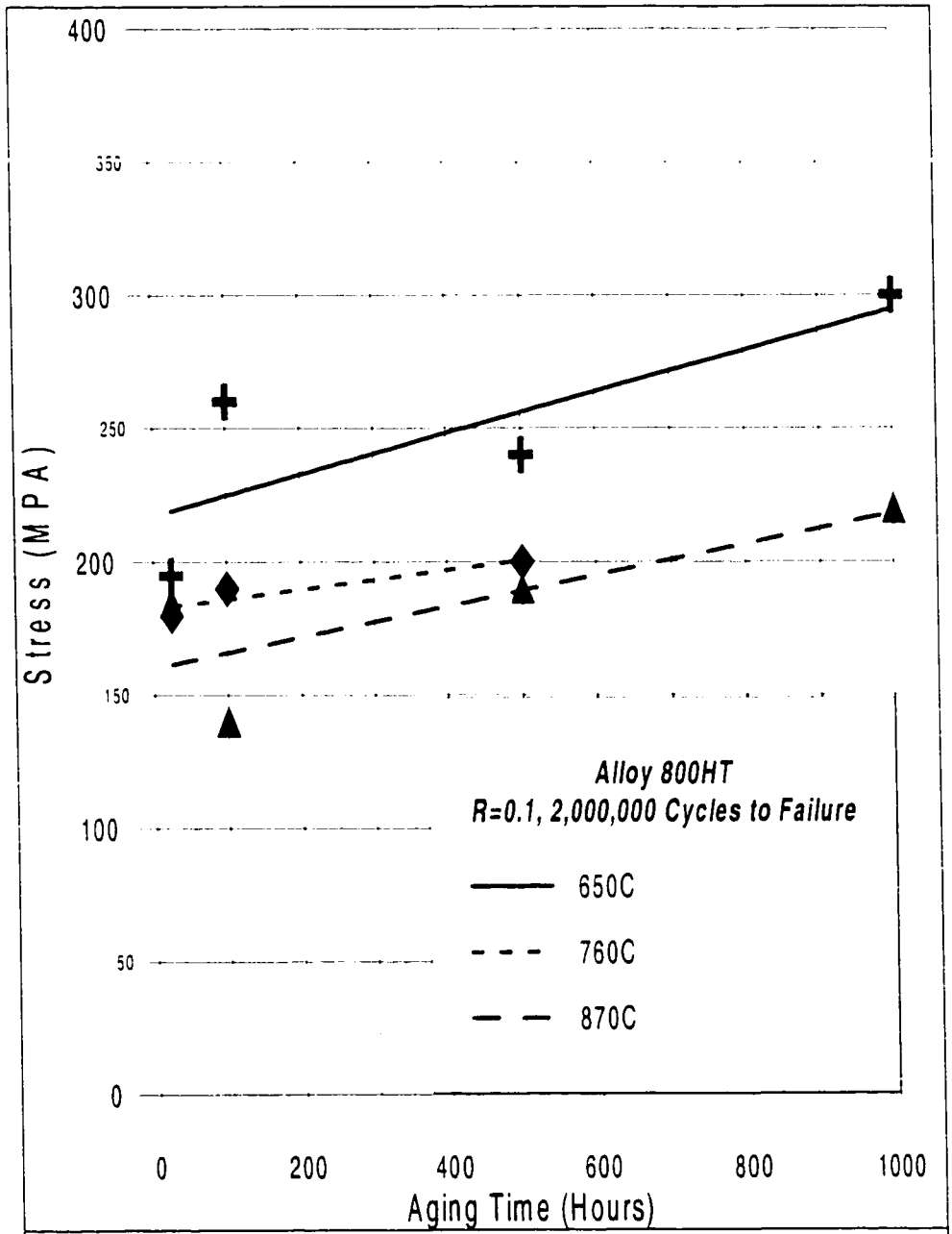

Figure 47: The effect of temperature on fatigue strength at N = 2,000,000.

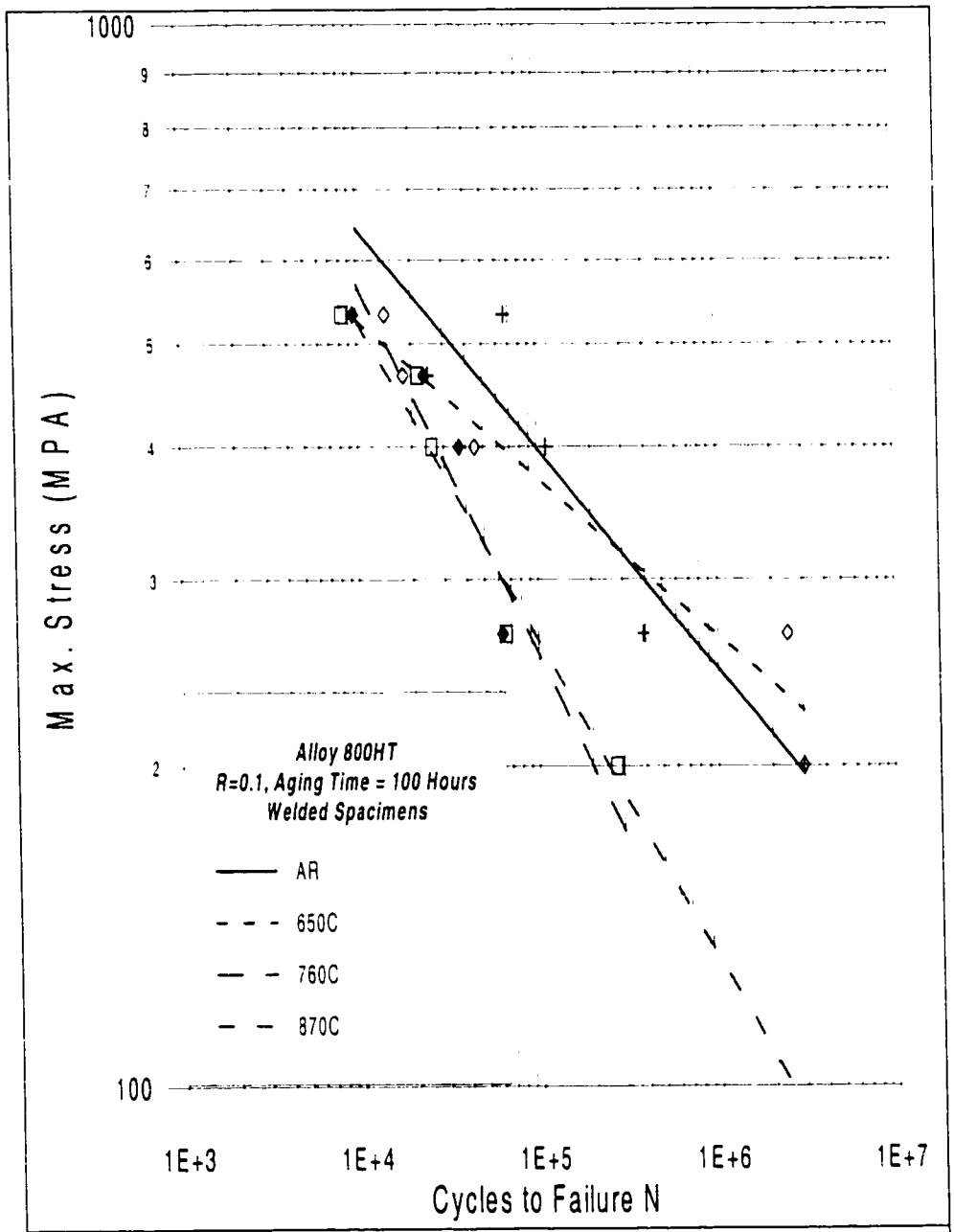

Figure 48: The effect of temperature on the fatigue strength after 100 hours aging time for welded specimens

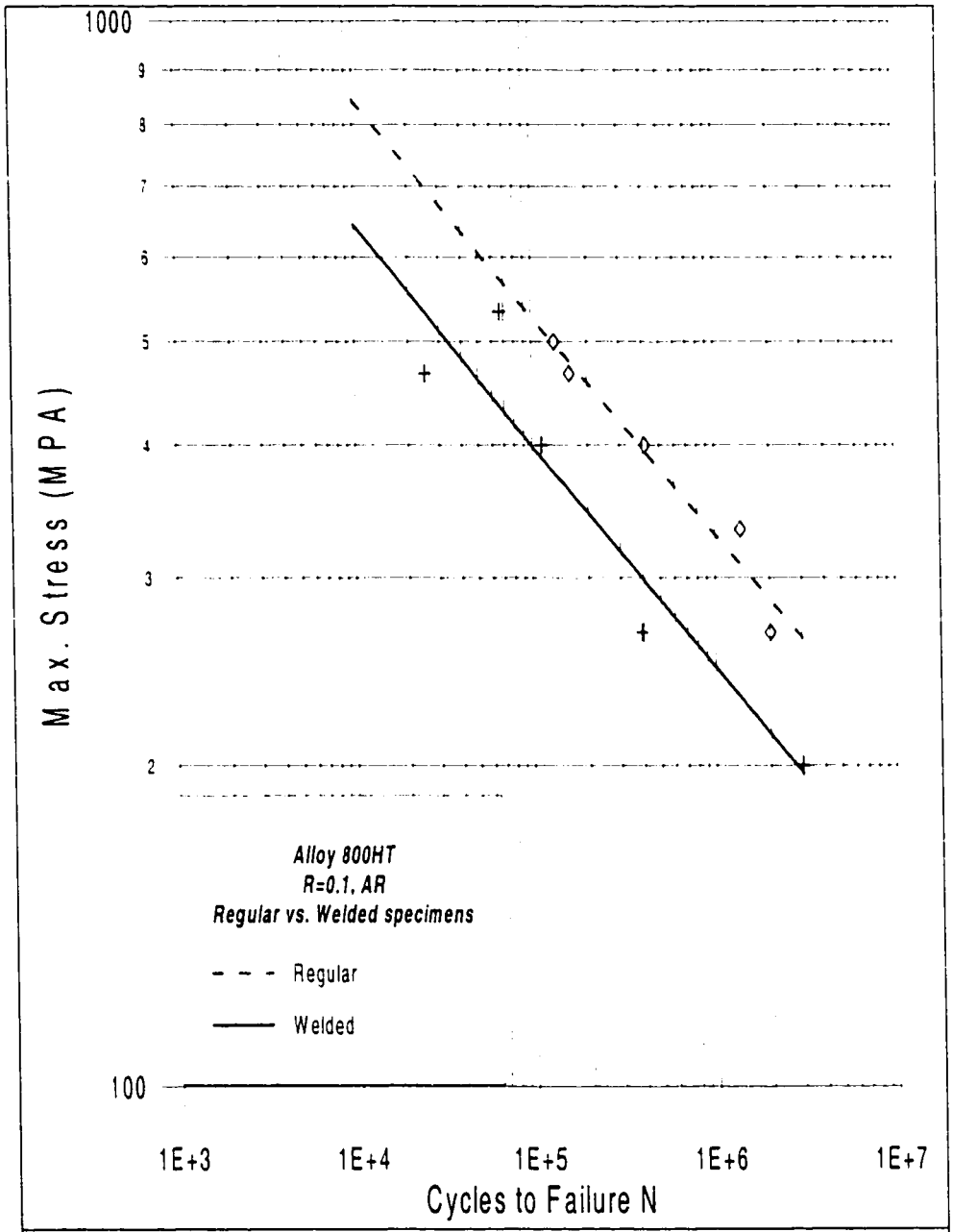

Figure 49: Fatigue strength of as-received specimens (welded vs. regular)

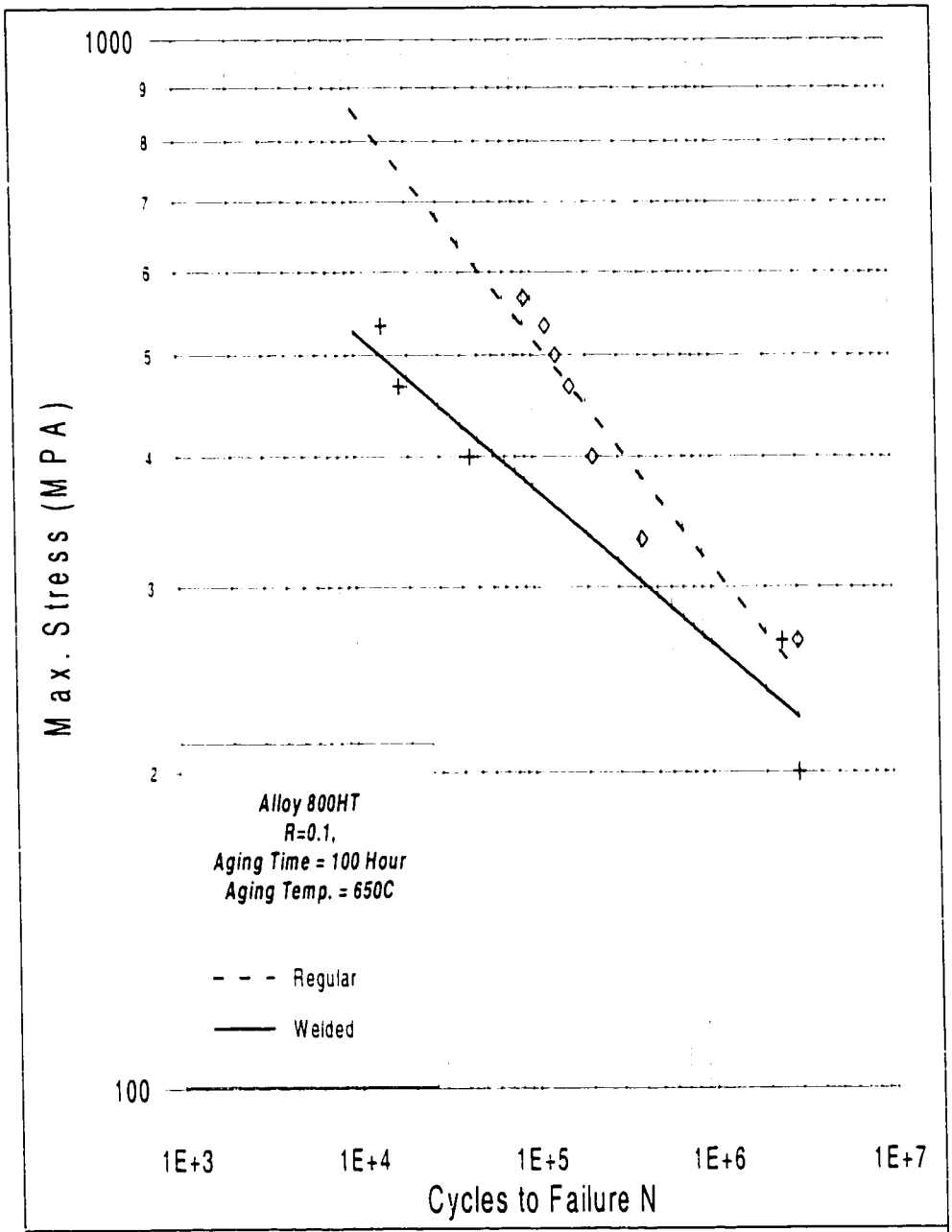

Figure 50: Fatigue strength of specimens aged at 650°C for 100 hours (welded vs. regular)

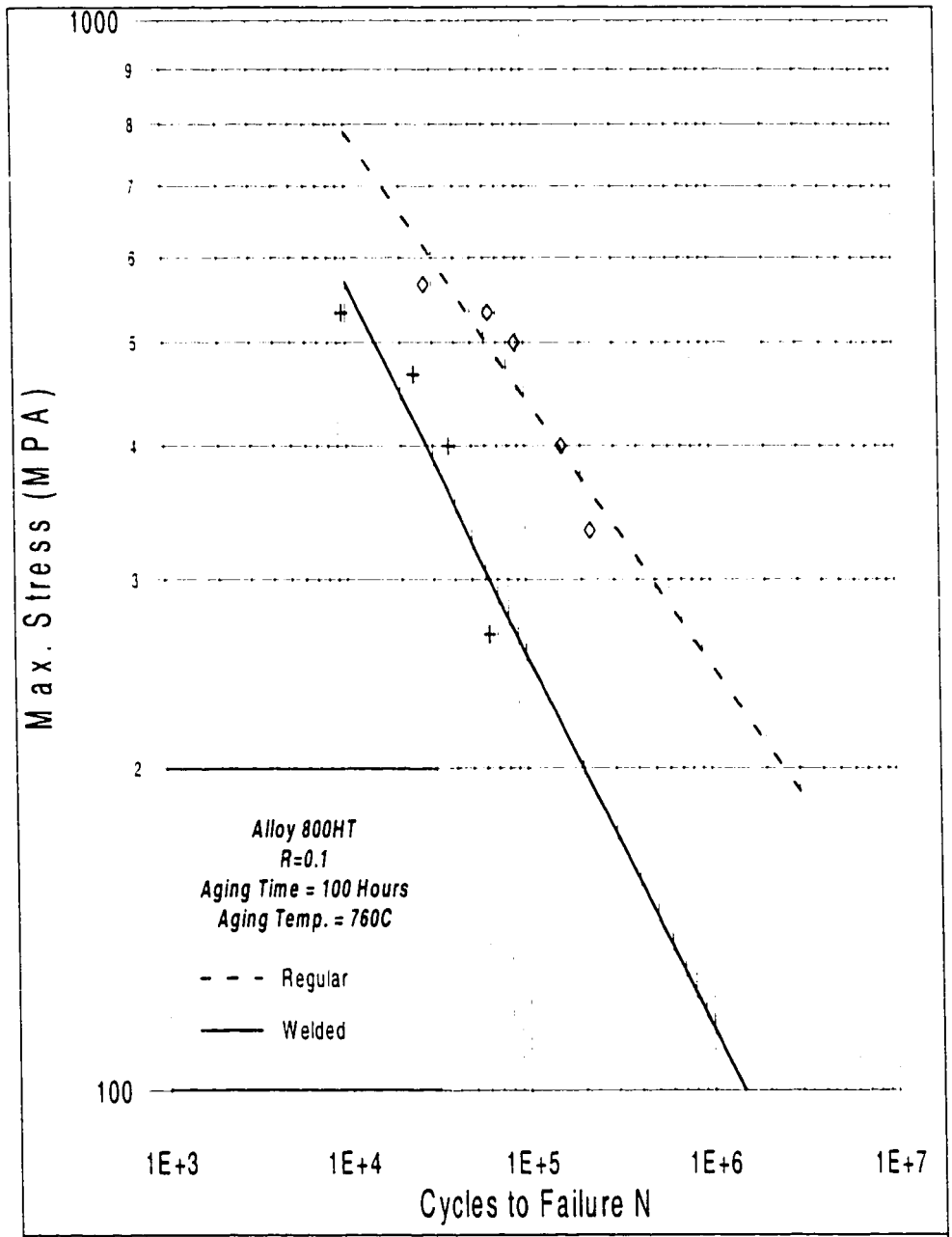

Figure 51: Fatigue strength of specimens aged at 760°C for 100 hours (welded vs. regular)

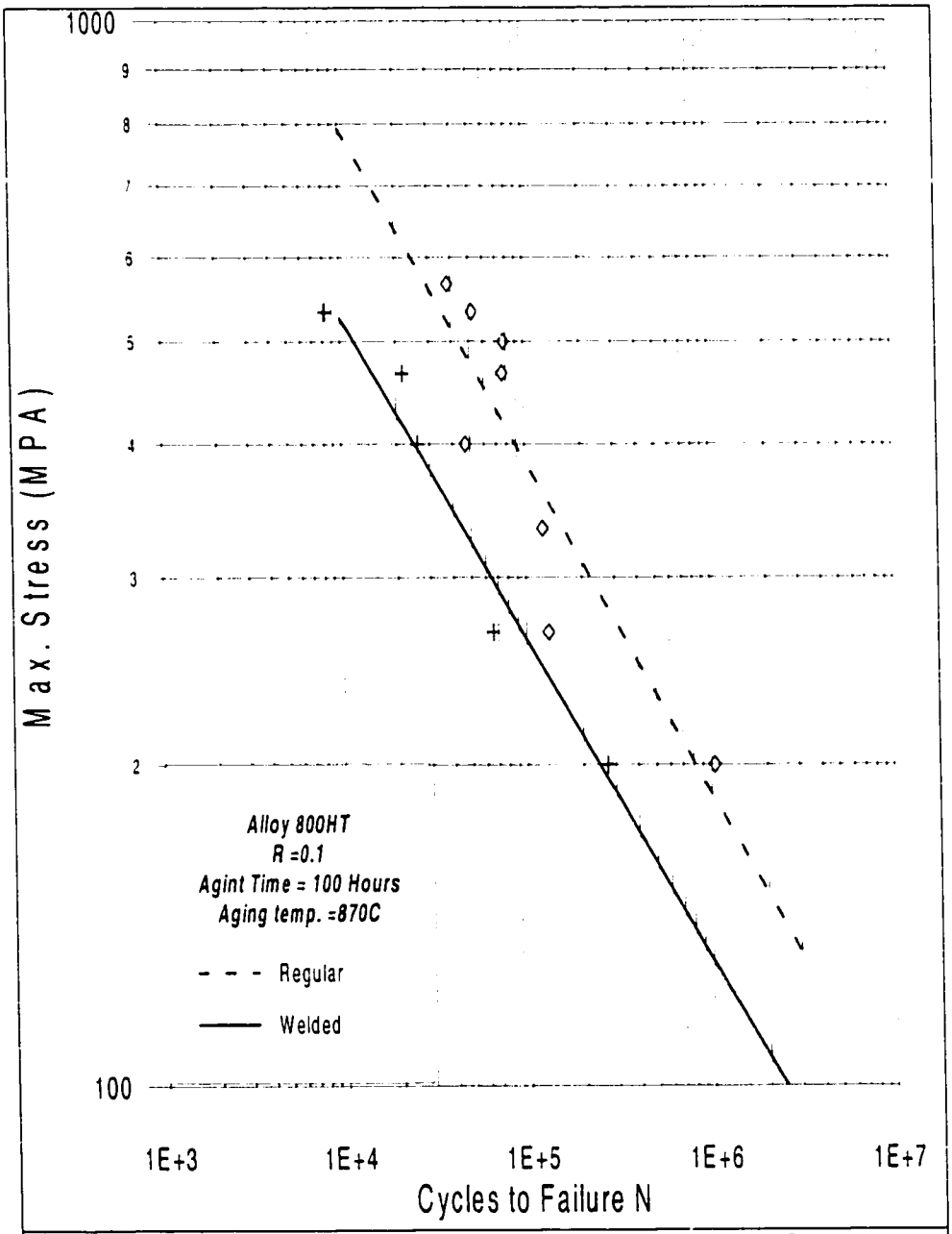

Figure 52: Fatigue strength of specimens aged at 870°C for 100 hours (welded vs. regular)

References

1. K. Y. HOUR and J F. STUBBINS, "The Effects of Hold Time and Frequency on Crack Growth in Alloy 800H at 650 C", Metallurgical Transactions A, Vol. 20A, September 1989, 1727-1734.

2. "Incoloy Alloys 800 and 800HT", published by Inco Alloy International, Huntington, USA, 1993.

3. "Product Handbook", published by Inco Alloys International, Huntington, USA, 1996.

4. W. L. MANKINS and S. LAMB, "Nickel and Nickel Alloys", Metals Handbook, 8th Edition, Volume 1, 1961.

5. D. A. DEANTONIO, T. HOWSON and M. F. ROTHMAN, "Heat Treating of Superalloys", Metals Handbook, 8th Edition, Volume 2, 1964.

6. W. H. KEARNS, "Metals And Their Weldability", Welding Handbook 7th Edition, Vol. 4, pp. 236.

7. S. D. ANTOLOVICH and A. SAXENA, "Fatigue Failure", Metals Handbook, 8th Edition Volume 10, 1975.

8. C. R. BRINKMAN", High-Temperature Time-Dependent Fatigue Behavior Of Several Engineering Structural Alloys", International Metal Reviews, Vol. 30, No. 5, 1985, pp. 235-258.

9. E. EL-MAJD, G. NICOLINI, and M. FARAG", Effect Of Carbide Precipitate On Creep Behavior Of Alloy 800HT In The Temperature Range 700°C To 900°C", Metallurgical And Materials Transactions A, Vol. 27A, March 1996, pp. 747-756.

10. K. BHANU SANKARA RAO, H. SCHUSTER, and G. R. HALFORD, "Mechanism Of High Temperature Fatigue Failure In Alloy 800H", Metallurgical and Materials Transactions A, Vol. 27A, April 1996, pp.851-861.

11. A. PLUMTREE and J. O. NILSSON, "High Temperature Fatigue Damage In Three Austenitic Alloys", Fatigue Fract. Engng. Mater. Struct., Vol. 11 No. 5, 1988, pp. 397-407.

12. K. BHANU SANKARA RAO, H. SCHIEFFERS, H. SCHUSTER, and G. R. HALFORD, "Temperature and Strain Rate Effects on Low-Cycle Fatigue Behavior Of Alloy 800H", Metallurgical And Materials Transactions A, Vol. 27A, February 1996, pp. 255-267.

13. C. P. HUNTER, R. C. HURST, and D. M. TAPLIN, "Creep Crack Growth Studies on alloy 800H Tubes Under Complex Loading Conditions", Materials At High Temperatures, Vol. 10 No. 2, May 1992, pp. 144-149.

14. Z. MU, K. BOTHE, and V. GEROLD, "Damage Mechanism In Alloy 800H Under Creep-Fatigue Conditions", Fatigue Fract. Engng. Mater. Struct., Vol. 17, No. 5, 1994, pp.523-537.

15. A. MIGNONE, M. F. MADAY, A. BORELLO, and M. VITTORI, "Effect Of Chemical Composition, Thermal Treatment, And Caustic Concentration On SCC Behavior Of Alloy 800", Corrosion, Vol. 46, No. 1, 1990, pp.57-65.

16. M. RODIG, H. HUTHMANN and W. HARTNAGEL, "Fatigue And Creep Crack Growth Of Alloy 800 And Alloy 617 At High Temperatures", Materials At High Temperatures, Vol. 10, No. 4, 1992, pp.268-274.

17. G. E. DIETER, " fatigue of metal", Mechanical Metallurgy, 1988, pp.375-431.

18. P. SOO, and R. L. SABATINI, "High-Cycle Fatigue Behavior Of Incoloy Alloy 800h In A Simulated HTGR Helium Environment Containing High Moisture Levels", Nuclear Technology, Vol. 66, 1984, pp.324-346.

19. K. BHANU SANKARA ROA, M. VALSAN and S. L. MANNAN, "Strain-controlled Low Cycle Behavior of Type 304 Stainless Steel Base material, Type 308 Stainless Steel Weld Metal and 304-308 Stainless Steel Weldments", Material Science and Engineering, A130 (1990), pp.67-82.

20. T. WAKAI, M. SAKANE, M. OHNAMI, K. OKITA AND Y. FUKUCHI, "High temperature Low-Cycle Fatigue of Friction Welded Joints-Type 304-304 Stainless Steel and Alloy 718-718 Nickel base Superalloy", Journal of engineering Material and Technology, Vol. 115, January 1993, pp.109-115.

VITA

Fathi H. AlHabib obtained his Bachelor of Science degree in Mechanical Engineering in 1986 from New Mexico State University at Las Cruces, New Mexico, USA. In 1986, he joined ARAMCO and worked as a Mechanical Engineer in Project Inspection and Consulting Services Departments. Mr. AlHabib joined the Aluminum Producing Co. (ALUPCO) in 1993 as a production engineer in the Aluminum Extrusion Plant. He joined the National Methanol Company (IBN SINA) in 1996 where he is presently working as a Project Engineer.